

Observations of Gulf Stream-Induced and Wind-Driven Upwelling in the Georgia Bight Using Ocean Color and Infrared Imagery

CHARLES R. MCCLAIN

Goddard Laboratory for Atmospheric Sciences, NASA Goddard Space Flight Center

LEONARD J. PIETRAFESA

Department of Marine, Earth and Atmospheric Sciences, North Carolina State University

JAMES A. YODER

Skidaway Institute of Oceanography

Ocean color and infrared imagery from aircraft and satellite sensors are combined with in situ measurements of currents, chlorophyll, temperature, salinity, coastal winds, and sea level to study upwelling events in the Georgia Bight where the Gulf Stream and continental shelf waters strongly interact. These interactions were observed over an 8 day period in April 1980 during which five independent upwellings occurred. The upwellings included a nearshore wind-driven upwelling enhanced by topographic effects, three Gulf Stream filament-induced upwellings, and what appears to have been a Gulf Stream meander-induced event. The chlorophyll distributions as inferred from the imagery are found to be reliable tracers which indicate filamentary circulation and propagation and advective routes by which nearshore water moves offshore. The propagation of two of the filaments and the meander are studied in detail using the imagery and mooring array temperature time series. Both techniques yield nearly identical results for the phase speeds of each event. There is evidence that one of the filaments accelerated as it entered into the Charleston Bump area where the Gulf Stream deflects offshore. The other filament exhibited a steady deceleration as it moved past Cape Canaveral and eventually lost any semblance of wave motion. Also included are data from April 1979 which offer corroborating evidence of filamentary structure and circulation. Intercomparisons of field measurements and the Nimbus 7/coastal zone color scanner estimates of surface pigment concentrations show excellent agreement over the range of 0.1-7.0 mg/m³.

1. INTRODUCTION

The investigation of mesoscale oceanic structure in the South Atlantic Bight (SAB) using conventional techniques has proven to be difficult due to the temporal and spatial variability of the region's dynamical processes. Satellite infrared (IR) imagery has been extremely useful for observing the Gulf Stream in this region, and a more recently developed technique, ocean color (visible) imagery, promises to be an invaluable tool in both physical and biological oceanography. In this report, Gulf Stream frontal upwellings in the Georgia Bight are discussed. The Georgia Bight spans the northeast Florida and Georgia shelves. Emphasis is placed on the observations made during the period of April 11-18, 1980. During this time, a sequence of five scenes from the Nimbus 7/coastal zone color scanner (CZCS) was collected. Additional data from filaments observed during April 1979 are included. The CZCS imagery is supplemented with imagery from the U-2/ocean color scanner (OCS), the airborne thematic mapper simulator (TMS), and NOAA frontal analyses from the AVHRR (advanced very high resolution radiometer). Each frontal feature had unique patterns of sea surface temperature and chlorophyll. By combining the imagery, hydrographic, and biological survey data, wind, sea level, and current information with conceptual flow models, explanations for the various surface pigment and temperature patterns observed are developed.

This paper is not subject to U.S. copyright. Published in 1984 by the American Geophysical Union.

Paper number 4C0025.

1.1. Ocean Color Remote Sensing

The qualitative dependence of the ocean's upwelled radiance spectrum on surface-layer chlorophyll concentration using airborne remote measurements was demonstrated by Clarke *et al.* [1970]. Because chlorophyll and phaeophytin pigments have similar absorption peaks near 440 nm, the blue portion of the upwelled spectrum is suppressed as concentration is increased. There are many other substances such as sediments and gelbstoff (yellow substance) which influence the subsurface reflectance through absorption and scattering, but in the open ocean, absorption by photosynthetic pigments is primarily responsible for variability in the ocean's albedo. Clarke *et al.* showed that as the measurement altitude increased, the total amount of light scattered upward by the atmosphere increased and eventually dominated the spectrum, thus masking the ocean's signature. This path radiance is strongly wavelength dependent and is composed of the Rayleigh component due to gas molecules and the aerosol component from suspended particulates. The first is readily calculated, but the second is much more difficult because aerosol concentrations are highly variable and their scattering and absorption characteristics are not well known.

In the early 1970's, NASA began the development of scanning radiometers (see Table 1) designed to image changes in the upwelled visible spectrum with channels located at the absorption maxima and minima of various pigments. One prototype instrument was the U-2/ocean color scanner (OCS), which is described in Kim *et al.* [1980]. In October 1978 the first satellite-borne ocean color scanner, the Nimbus 7 coastal

TABLE 1a. Scanner Characteristics: Instrument, Resolution, and Swath Width

Instrument	Resolution,* m	Swath Width, km
TMS	16	15
U-2/OCS	70	40
CZCS	825	1600

*Size of nadir pixel at ground level.

TABLE 1b. Scanner Characteristics: Center Wavelength/Bandwidth

Channel	OCS	CZCS	TMS
1	431/24	443/20	485/70
2	472/26	520/20	560/80
3	506/25	550/20	660/60
4	548/26	670/20	830/140
5	586/24	750/100	1150/300
6	625/25	11500/2000	1650/200
7	667/24		2220/270
8	707/26		11500/2100
9	738/24		
10	778/26		

*In nanometers.

zone color scanner (CZCS), which is discussed by *Hovis* [1981], was launched into a sun-synchronous orbit. The primary objective of the CZCS mission was to develop the capability to estimate reliably surface pigment concentration from a space platform. To achieve this goal, algorithms for both atmospheric corrections and for relating water radiance spectra to pigment concentration (bio-optical algorithms) had to be developed. Several approaches to the first problem have been suggested. The most successful for application to the CZCS are those by *Smith and Wilson* [1981] and by *Gordon et al.* [1983]. As for the pigment algorithms, those by *Gordon and Clark* [1980] and *Morel* [1980] are two of the most well known. *Sturm* [1981] compared various algorithms using CZCS data and demonstrated that the derived products can

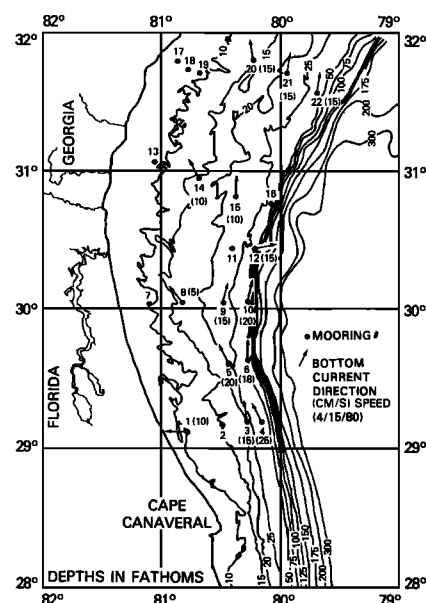


Fig. 1. Georgia Bight bathymetry, the GABEX-I mooring array and bottom flow vectors on April 15, 1980.

deviate significantly. Nonetheless, in a recent study of pigment distributions in a warm core ring by *Gordon et al.* [1982], the rms value of the ratio of the difference between ship and satellite concentrations to the ship measurements was only 0.36.

1.2. Upwelling Processes in the Georgia Bight

The dynamics of the outer continental shelf of the Georgia Bight are dominated by the Gulf Stream. In this region, the Gulf Stream strongly interacts with the bottom topography as shown in Figure 1 and does not deviate far from the shelf break except farther downstream in the vicinity of the Charleston Bump where it is sharply deflected offshore near 32°N [*Brooks and Bane*, 1978; *Pietrafesa et al.*, 1978; *Rooney et al.*, 1978; *Chao and Janowitz*, 1979]. Associated with the front are meanders and filaments which are frontal waves, but the terminology is loosely defined in the literature. To avoid

TABLE 2. Summary of Observations of Northward Propagating Waves in the SAB

Wavelength, km	Period, days	Phase Speed, cm/s	Location	Source
200	5	47	S.E. Florida	<i>Düing</i> [1975]
129	2.3	65	S.E. Florida	<i>Lee and Mayer</i> [1977]
263	3.1	98		
160	9.3	39		
265	7.8	39	Georgia Bight	<i>Legeckis</i> [1975]
...	3.5	...	Georgia Bight	<i>Lee et al.</i> [1981]
225	6.2	42		
...	10	...		
...	2	...	Georgia Bight	<i>Lee and Atkinson</i> [1983]
...	2.5	...		
...	8	55		
...	3	...		
...	3.9	...	Carolinas	<i>Webster</i> [1961]
...	6.9	...		
177	4.6	45	Carolinas	<i>Legeckis</i> [1979]
148	6.2	28	Carolinas	<i>Vukovich and Crissman</i> [1980]
115	3.7	36		
...	3.3	...	Carolinas	<i>Brooks and Bane</i> [1981]
230	7.4	36		
...	...	54*		
204	6.1	39	Carolinas	<i>Bane et al.</i> [1981]

*Average value for entire subinertial range.

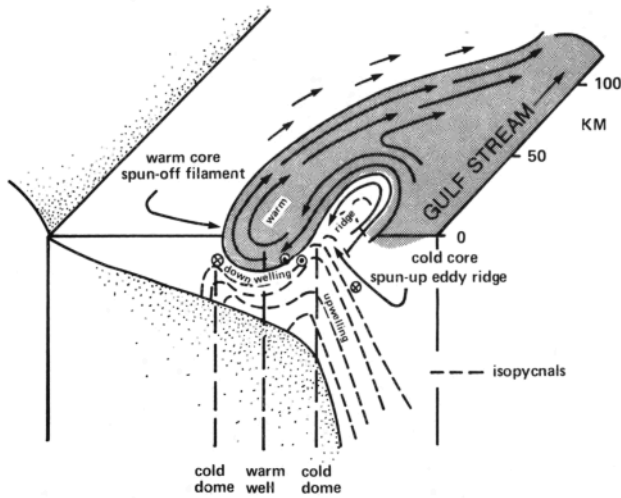


Fig. 2. Conceptual Gulf Stream filament structure and circulation.

confusion, filaments or shingles are considered to be nonlinear highly skewed waves, while meanders are smaller amplitude waves that are not folded double. *Orlanski* [1969] related the evolution and propagation of meanders having small across-shelf amplitudes and long wavelengths in the Gulf Stream to bottom topography and stratification. He predicted that typical baroclinic waves for this section of the Gulf Stream would have wavelengths ≈ 226 km and phase speeds of 23–38 cm/s. The most unstable northward propagating barotropic wave for this region, as was predicted by *Niiler and Mysak* [1971], has a wavelength of 140 km and a phase speed of 16 cm/s. Some evidence exists which indicates that the phase speeds of these waves may increase as they propagate to the north [*Le-*

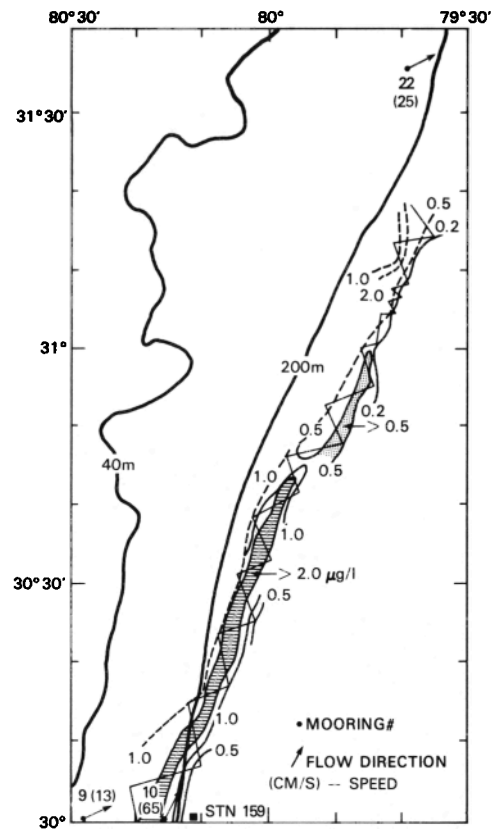


Fig. 4. Surface chlorophyll map from the *Columbus Iselin* survey, April 15–16, 1980. Dashed line contours represent chlorophyll isopleths within shelf waters, whereas solid lines are isopleths within Gulf Stream water.

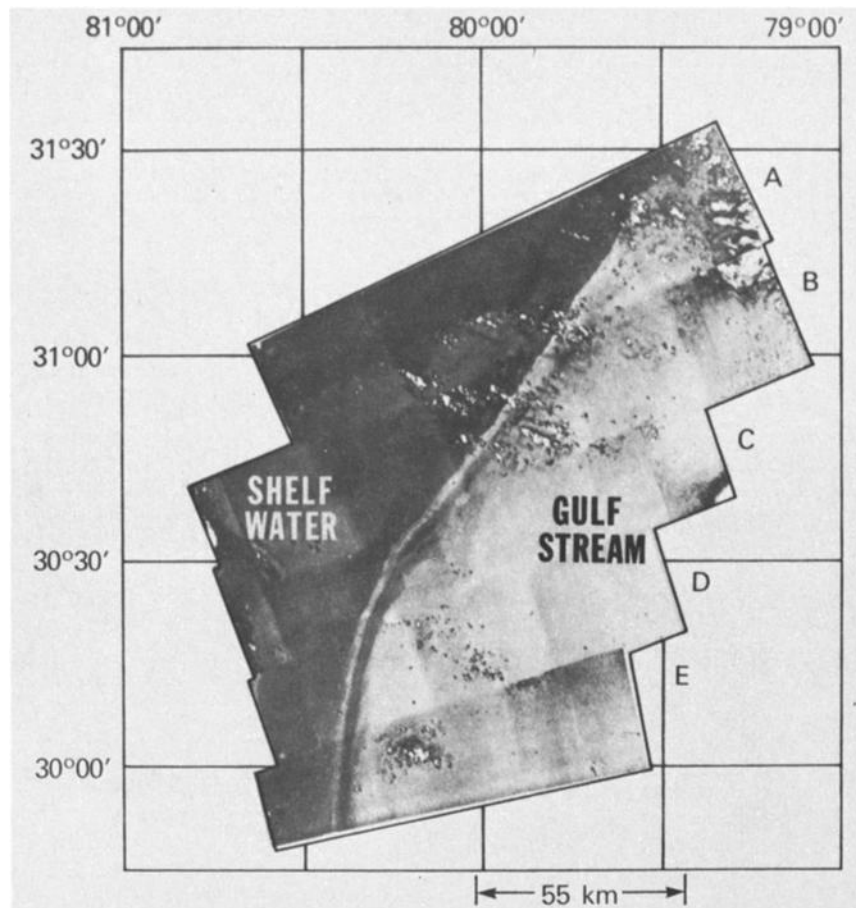


Fig. 3. U-2/OCS composite image, April 15, 1980.

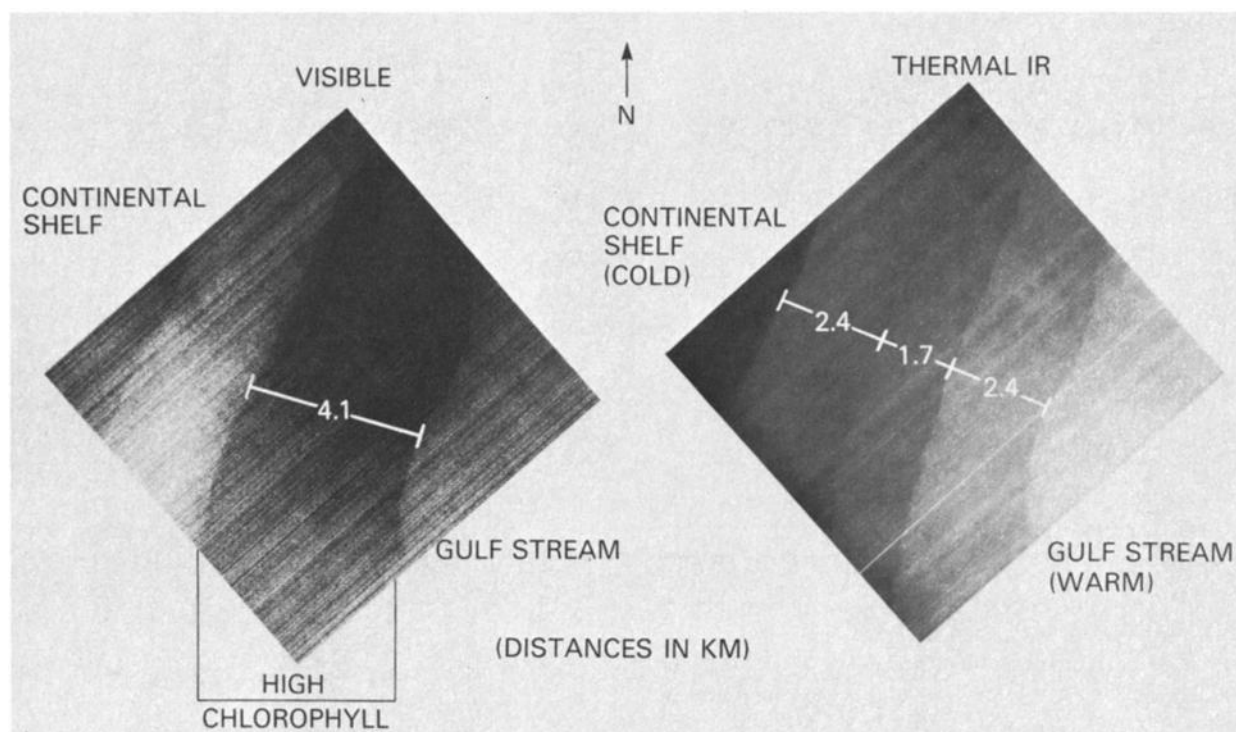


Fig. 5. TMS imagery of Gulf Stream frontal divergence zone, April 15, 1980.

geckis, 1975; Vukovich and Crissman, 1980] and that there is seasonal and interannual variability in their characteristic wavelength [Legeckis, 1979]. The average wave amplitude north of the Charleston Bump is approximately twice the amplitude to the south [Bane and Brooks, 1979]. Table 2 is a summary of observations of Gulf Stream wave properties in the SAB.

Both meanders and filaments are rather complex structures, and the detailed circulation within them is not clearly understood. Discussions on filamentary circulation are found in Lee [1975], Pietrafesa and Janowitz [1979, 1980], Lee et al. [1981], Chew [1981], Brooks and Bane [1981], Bane et al. [1981], Sun [1982], Chew et al. [1982], Pietrafesa [1983], and Lee and Atkinson [1983]. The conceptual flow field proposed by Pietrafesa and Janowitz [1980] is shown in Figure 2. The salient aspects of their model are the domed ridge of upwelled

water called the "cold core," the cyclonic circulation within the cold core, and the anticyclonic flow within the "warm tongue." All investigators agree that upwelling of Gulf Stream water occurs in the cold core, and the biological response to this upwelling is documented in Kim et al. [1980] and in Yoder et al. [1981]. An issue is whether the flow in the warm tongue is entirely to the south [Lee et al., 1981] or reverses and flows northward as shown in Figure 2. Flow reversal in the warm tongue is supported by Chew [1981] based on vorticity considerations, by the numerical model results of Sun

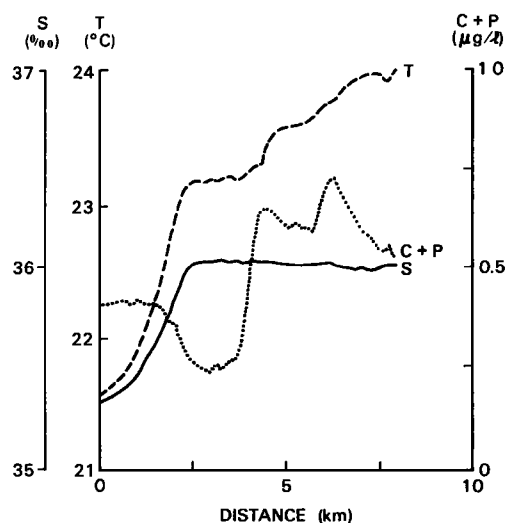


Fig. 6. Sea surface temperature, salinity and pigment profiles across the Gulf Stream frontal divergence zone from a Columbus Iselin transect, April 15, 1980.

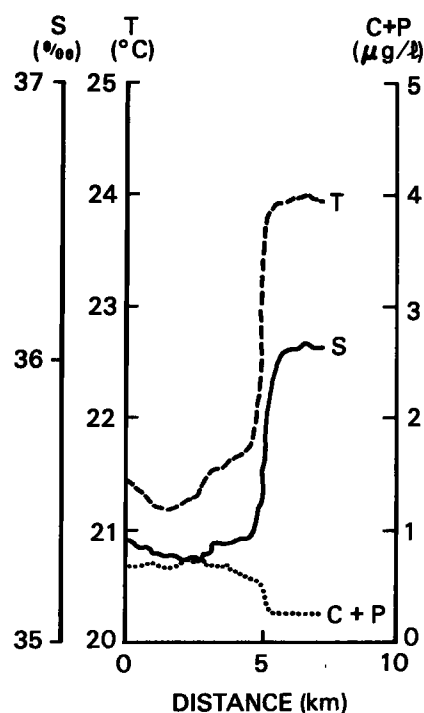


Fig. 7. Sea surface temperature, salinity, and pigment profiles across the meander trough from a Columbus Iselin transect, April 15, 1980.

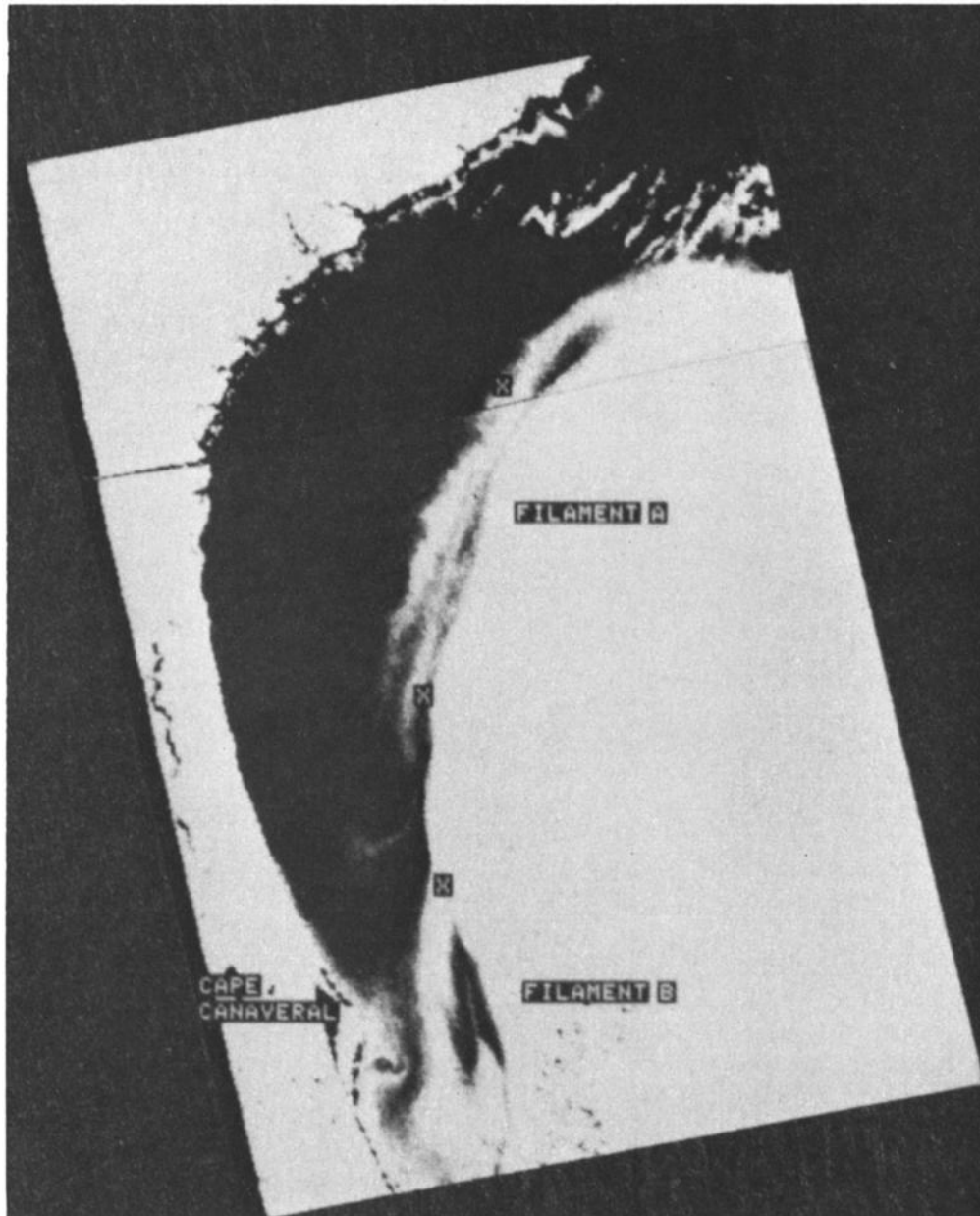


Fig. 8a. CZCS visible image on April 11, 1980, with moorings 4, 10, and 22 located.

[1982], and by Pietrafesa and Janowitz [1979] and Pietrafesa [1983] based on combined satellite and current meter observations. On the other hand, Lee *et al.* [1981] and Lee and Atkinson [1983] conclude that there is no evidence of anticyclonic motion in filaments based on similar types of data. It may well be that both arguments can be correct under certain conditions of bathymetry, wind forcing, etc. However, the filament discussed in Lee and Atkinson [1983] and Pietrafesa [1983] is the same event, and the differing interpretations appear to be due to different analyses of the current meter data, Lee and Atkinson having band-pass filtered the data, while Pietrafesa only low-pass filtered it.

Meanders are structurally less complicated than filaments and, in an Eulerian sense, appear as onshore/offshore excursions of the front with simultaneously increasing/decreasing surface temperature. The intrusion of Gulf Stream water across the continental shelf has been discussed by a large

number of investigators including Blanton [1971], Stefansson *et al.* [1971], Atkinson [1977], Blanton and Pietrafesa [1978], Leming and Mooers [1981], and Hofmann *et al.* [1981] and is attributed to offshore Gulf Stream meandering and upwelling favorable winds. Subsequent studies have shown that intrusions are the dominant source of nutrients to the middle and outer shelf [Dunstan and Atkinson, 1976; Lee *et al.*, 1981; Lee and Atkinson, 1983], and Yoder *et al.* [1983] conclude that the primary production due to outer shelf upwelling processes may exceed that of the inner shelf. Earlier studies held that the production in these areas was insignificant when compared with inner shelf production.

Meander-induced upwelling of a different nature is discussed by Chew [1974] and Newton [1978]. According to them, zones of upwelling and downwelling occur in the vicinity of the wave crest and trough, respectively. The crest is the maximum onshore excursion of the front, and the trough is

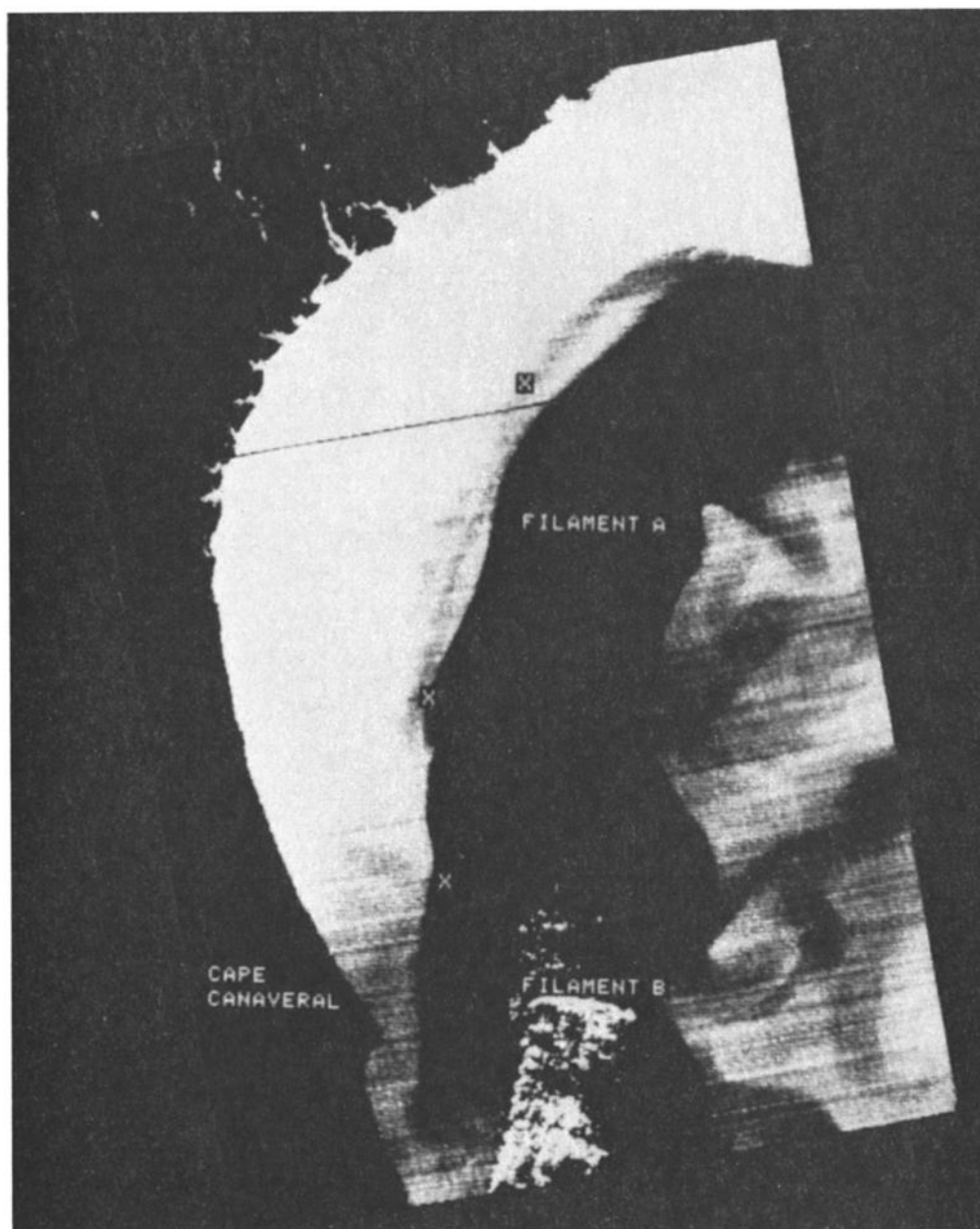
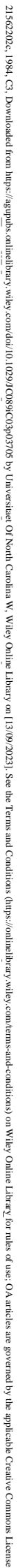


Fig. 8b. CZCS IR image on April 11, 1980, with moorings 4, 10, and 22 located.

the maximum offshore excursion. These motions are not to be confused with the bottom intrusions discussed above. Intrusion waters are derived from deeper depths. As will be shown later, the water associated with the crest upwelling originates from shallower depths near the subsurface chlorophyll maximum. The crest upwelling would be characterized by a relatively broad temperature gradient across the front, while the zone of surface convergence (downwelling) would produce a sharper, more well-defined front. For a simple gradient current, the spacing between isobaric surfaces in the radial direction is a function of the radius of curvature of the front which changes sign from crest to trough, thus decreasing the breadth of the front. Chew provides a detailed theoretical description with observations of the meandering process.

On the north Florida shelf, another type of upwelling due to current-bathymetry interaction can occur simultaneously with frontal wave-induced upwelling. In the theoretical work

of Hsueh and Ou [1975], shelf break upwelling is predicted when an alongshore current is present at the shelf break. In their model, alongshore bathymetric variations are not included, and the upwelling is solely a result of the β effect. However, in the Georgia Bight, alongshore bottom irregularities are important. According to the theory of Janowitz and Pietrafesa [1982], topographically induced upwelling and onshore flow will occur when a cyclonically sheared current encounters isobaths that diverge in the downstream direction. So, as the Gulf Stream flows past Fort Pierce, to the south of Cape Canaveral, the bathymetry begins to diverge and, in order to conserve potential vorticity, the flow deflects onshore resulting in a subsurface intrusion of Gulf Stream water onto the shelf. Further downstream at about 30°N , the isobaths begin to converge, and the flow deflects offshore. Their theoretical predictions are quantitatively consistent with field observations reported by Leming [1979] and Blanton *et al.* [1981].



21562022, 1984, C3, Downloaded from <https://agupubs.onlinelibrary.wiley.com/doi/10.1029/2018JC013705> by Universitat Of North Carolina W. Wiley Online Library on [13/09/2023]. See the Terms and Conditions (<https://onlinelibrary.wiley.com/terms-and-conditions>) on Wiley Online Library for rules of use. OA articles are governed by the applicable Creative Commons License

21562022, 1984, C3, Downloaded from <https://agupubs.onlinelibrary.wiley.com/doi/10.1029/2018JC013705> by Universitat Of North Carolina W. Wiley Online Library on [13/09/2023]. See the Terms and Conditions (<https://onlinelibrary.wiley.com/terms-and-conditions>) on Wiley Online Library for rules of use. OA articles are governed by the applicable Creative Commons License

21562022, 1984, C3, Downloaded from <https://agupubs.onlinelibrary.wiley.com/doi/10.1029/2018JC013705> by Universitat Of North Carolina W. Wiley Online Library on [13/09/2023]. See the Terms and Conditions (<https://onlinelibrary.wiley.com/terms-and-conditions>) on Wiley Online Library for rules of use. OA articles are governed by the applicable Creative Commons License

21562022, 1984, C3, Downloaded from <https://agupubs.onlinelibrary.wiley.com/doi/10.1029/2018JC013705> by Universitat Of North Carolina W. Wiley Online Library on [13/09/2023]. See the Terms and Conditions (<https://onlinelibrary.wiley.com/terms-and-conditions>) on Wiley Online Library for rules of use. OA articles are governed by the applicable Creative Commons License

21562022, 1984, C3, Downloaded from <https://agupubs.onlinelibrary.wiley.com/doi/10.1029/2018JC013705> by Universitat Of North Carolina W. Wiley Online Library on [13/09/2023]. See the Terms and Conditions (<https://onlinelibrary.wiley.com/terms-and-conditions>) on Wiley Online Library for rules of use. OA articles are governed by the applicable Creative Commons License

21562022, 1984, C3, Downloaded from <https://agupubs.onlinelibrary.wiley.com/doi/10.1029/2018JC013705> by Universitat Of North Carolina W. Wiley Online Library on [13/09/2023]. See the Terms and Conditions (<https://onlinelibrary.wiley.com/terms-and-conditions>) on Wiley Online Library for rules of use. OA articles are governed by the applicable Creative Commons License

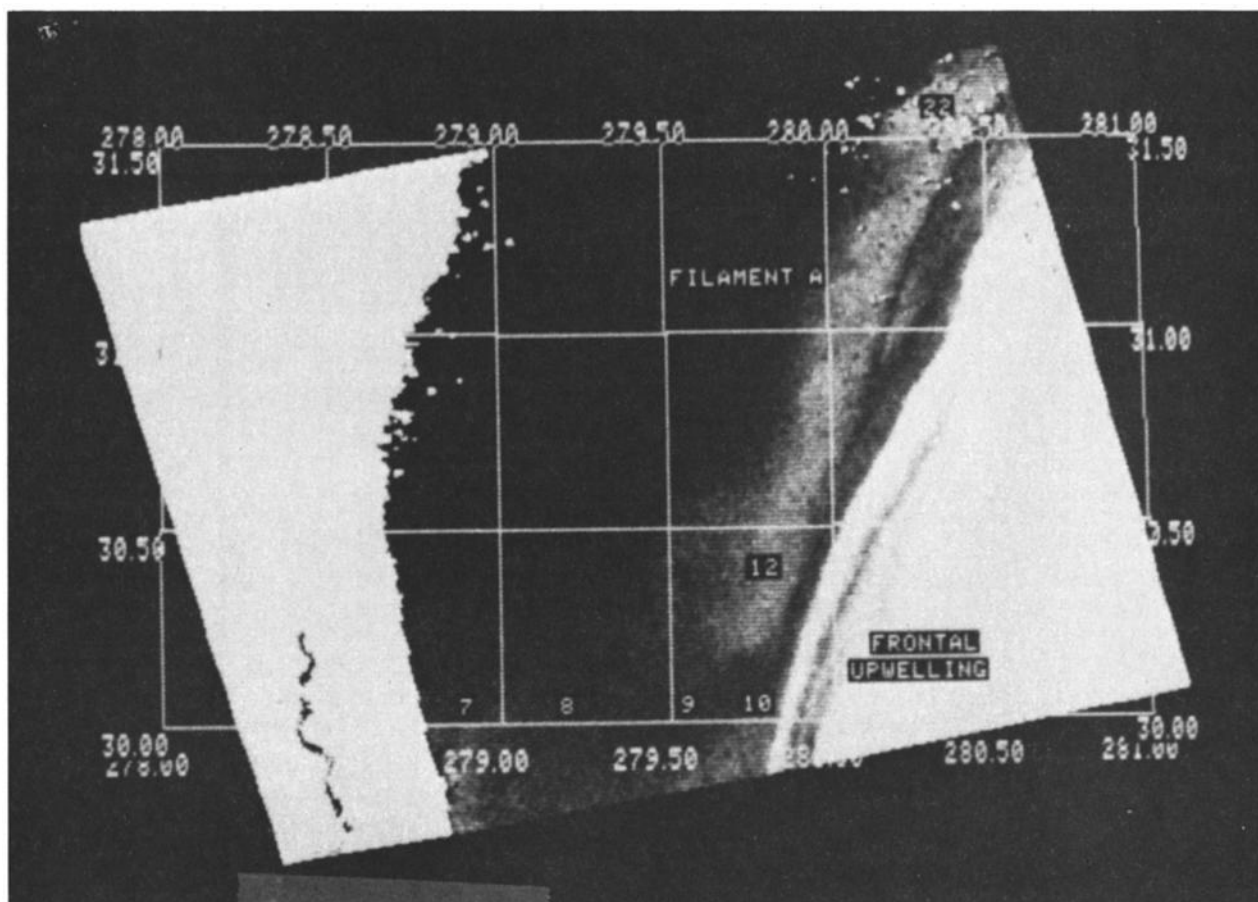


Fig. 10a. CZCS visible image on April 15, 1980, with mooring locations.

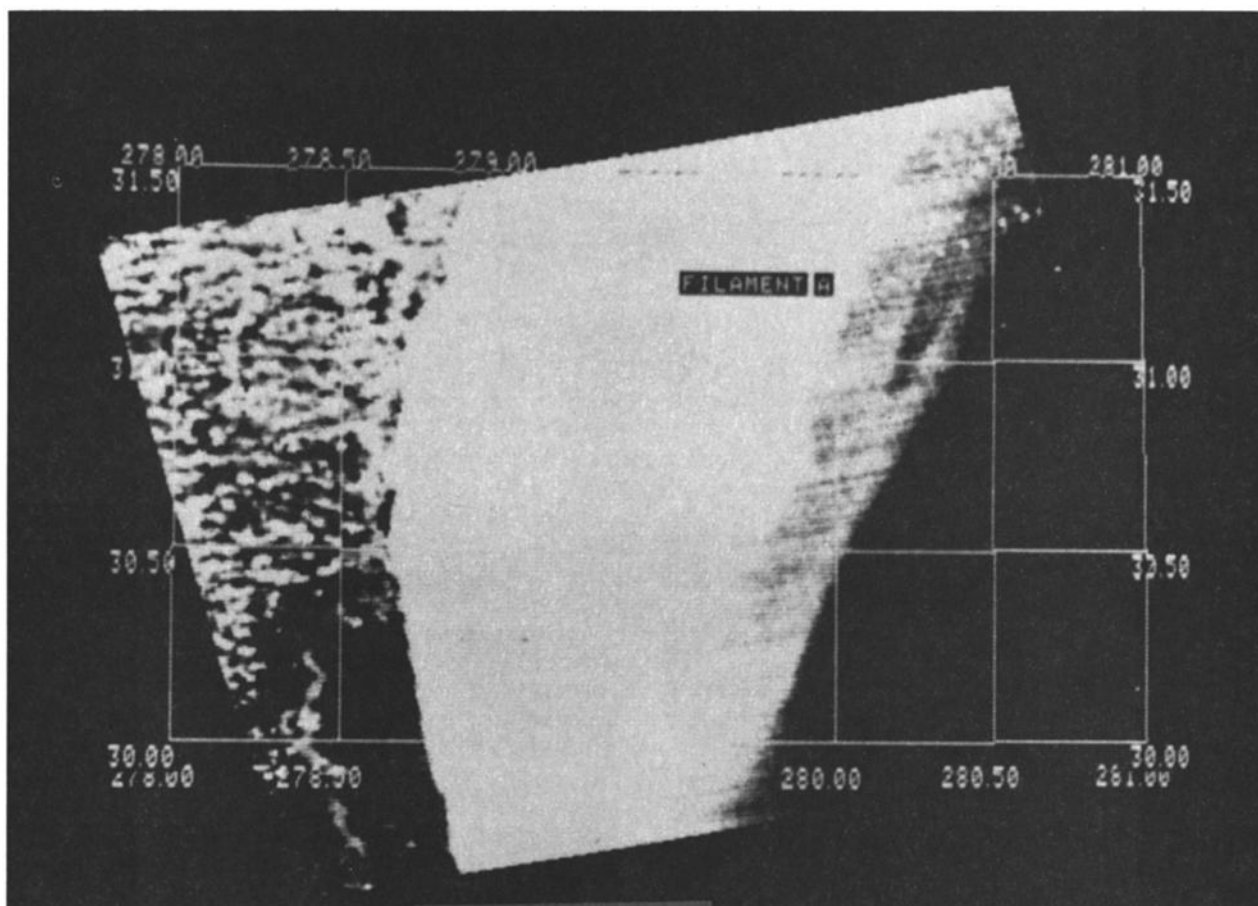


Fig. 10b. CZCS IR image on April 15, 1980, with mooring locations.

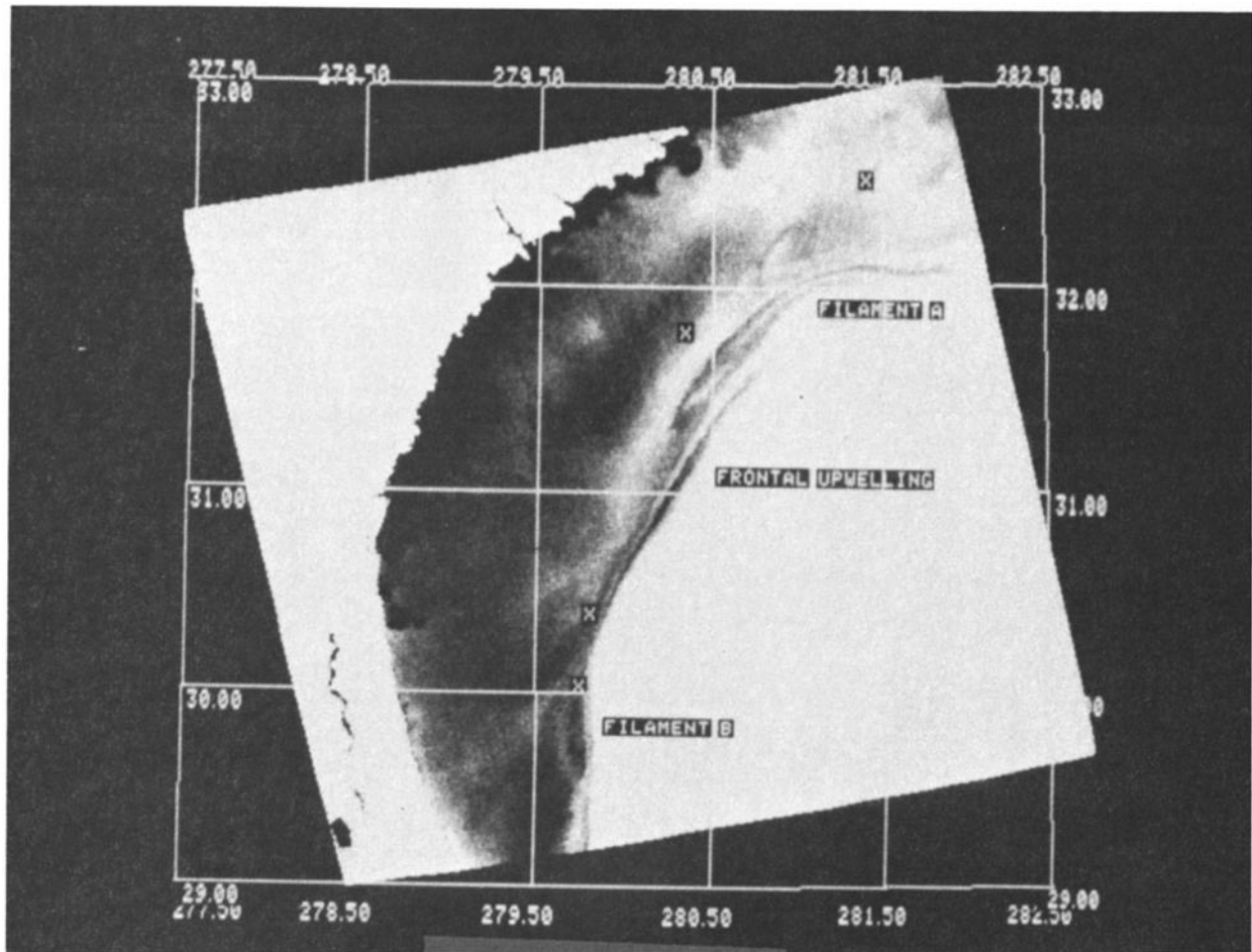


Fig. 11a. CZCS visible image on April 16, 1980, with moorings 10, 12, 22, and 25 located.

Stream frontal features as they propagated through the experiment site.

A U-2/OCS flight was conducted on April 15, and the composite image from the five tracks is shown in Figure 3. The darker tones represent areas of relatively high chlorophyll. The U-2 imagery shows the presence of a narrow alongshore band of high surface chlorophyll, which was separated from the shelf water by an interceding band of low chlorophyll. The northern terminus of the feature was roughly 31°N , but the southern boundary was beyond the aircraft coverage. The *Columbus Iselin* surface truth from April 15 and 16 is presented in Figure 4. The surface chlorophyll concentration as determined from continuous fluorometer measurements was as high as $7 \mu\text{g/l}$ in the plume. The two mappings are nearly identical in shape and location. Included in Figure 4 are current vectors from moorings 9 (7 m), 10 (7 m), and 22 (17 m). The near-surface currents at moorings 9 and 22 were offshore. For future reference, note the location of hydrographic station 159 in Figure 4. Also, referring back to Figure 1, the southern portion of the plumelike feature was located exactly over the shelf break at a location just north of where the shelf slope is the steepest.

Concurrent with the U-2 flight, a C-130 mission was flown, using the thematic mapper simulator (TMS). The swath of the TMS was much narrower since the C-130's altitude was only 6 km as compared to 20 km for the U-2. However, it has two compensating attributes, a resolution of 16 m at nadir instead

of 70 m and an IR channel. The TMS data were collected at roughly $31^{\circ}10'\text{N}$ and at $30^{\circ}20'\text{N}$. A portion of the southern flight track imagery is shown in Figure 5. The visible image (an enhancement of channel 1) shows the same structure as the OCS image and the *Columbus Iselin* surface map. The high chlorophyll band was approximately 4.1 km wide. The IR data indicate that the front was actually composed of a series of nearly isothermal mini-fronts with a staircase increase in temperature proceeding from the shelf to the Gulf Stream waters. The chlorophyll-rich area was associated with two adjacent isothermal bands. A *Columbus Iselin* transect of surface chlorophyll, temperature, and salinity across the structure is given in Figure 6. The ship transect proceeded to the east, and the rapid initial increases in SST and salinity indicate that the low chlorophyll and high chlorophyll bands were composed of Gulf Stream water, not shelf water. North of this bloom, the IR data from the TMS indicates that the front was very sharply defined in contrast to its structure further south. The *Columbus Iselin* transect (Figure 7) beneath this flight track corroborates the TMS data.

From the aircraft and *Columbus Iselin* information, it is not really possible to infer the source or the cause of the bloom. Therefore, CZCS images from April 11, 12, 15, 16, and 17 were obtained. Imagery from the 443 nm and IR channels from the first 4 of these days are provided in chronological order in Figures 8, 9, 10, and 11. No IR data from April 12 is included, and the scene from April 17 is of insufficient quality for pub-

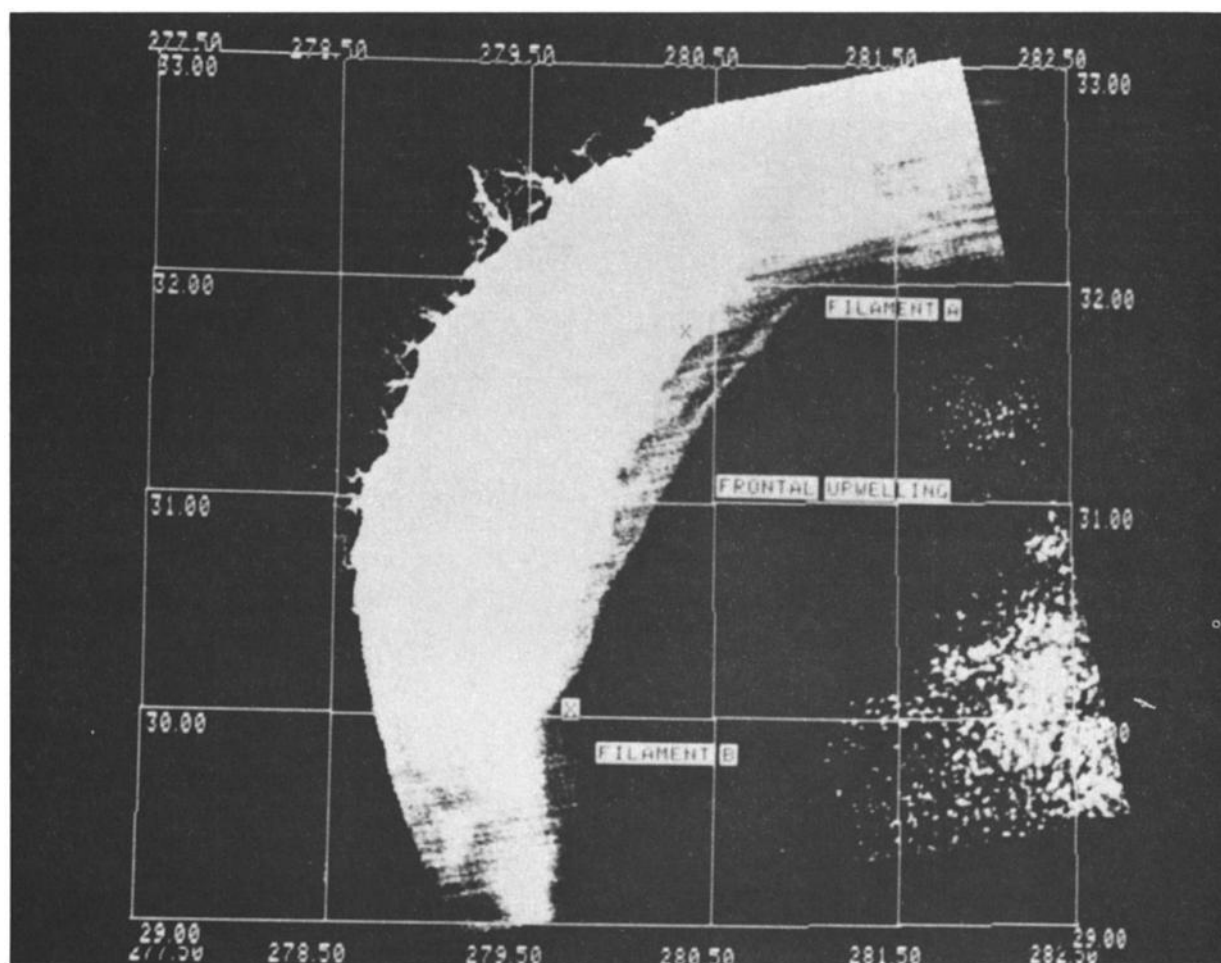


Fig. 11b. CZCS IR image, on April 16, 1980, with moorings 10, 12, 22, and 25 located.

lication. The 443 nm data has been corrected for atmospheric effects by using the “clear water radiance” technique [Gordon *et al.*, 1983]. The imagery on April 11 clearly shows that there were three filaments in the GABEX site. The two southernmost filaments are labeled A and B. That three filaments existed within the Georgia Bight at that time is also confirmed in the NOAA frontal analysis chart from April 14 (Figure 12). The SST signature of filament A on April 11 was weak, but a narrow cold core with relatively high pigment levels is evident as is the warm tongue (Figure 8). The warm tongue is more easily identified in Figures 10 and 11.

Hydrographic sections were made on April 15 by the *Columbus Iselin* and the *Eastward*. The *Columbus Iselin* section was completed prior to conducting the frontal mapping shown in Figure 4. The locations of these transects are shown in Figure 13. Figure 13 provides the temperature sections from the two transects. Although the *Columbus Iselin* continued across the shelf and into the Gulf Stream, vertical temperature profiles were discontinued near the 140-km point in the vicinity of filament A. The last CTD cast was at 110 km so there is no subsurface salinity data beyond that point. The temperature section indicates a doming of isopycnals at the shelf break, but it is unclear as to what comprised the near-surface water mass above mooring 22. The imagery in Figures 10 and 11 indicate relatively low pigment concentrations in that water mass. No fluorometer data were collected during the transect, so the pigment distribution of filament A was not in situ sampled.

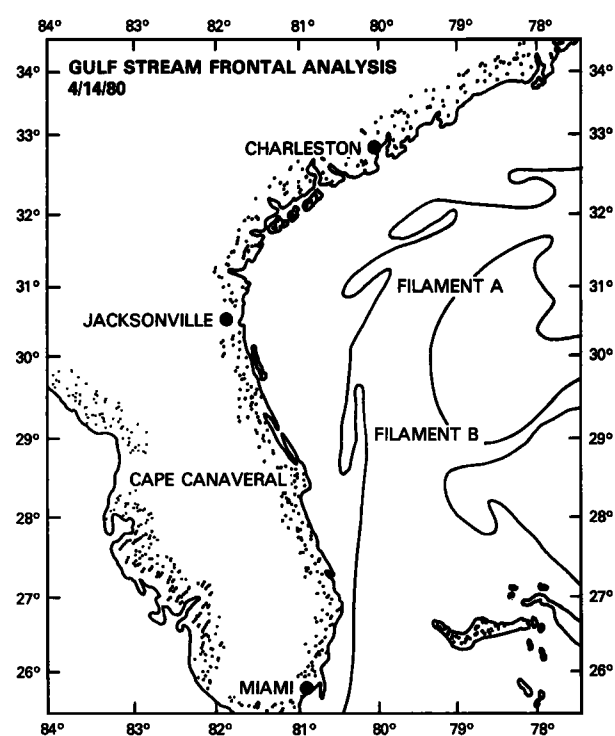


Fig. 12. NOAA frontal analysis chart on April 14, 1980. Courtesy of S. Baig, NOAA/AOML.

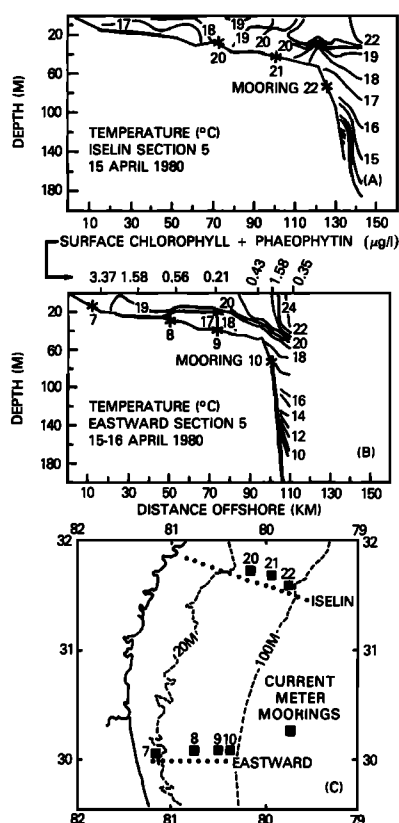


Fig. 13. Temperature sections on April 15, 1980 (a) *Columbus Iselin*, (b) *Eastward*, and (c) transect locations. Surface chlorophyll concentrations are indicated at the top of Figure 13b.

Fluorometer measurements commenced after the frontal mapping started. Judging from Figure 10, the surface signature of filament A may have been masked somewhat by fresher, cooler shelf water being entrained into the front north of filament B. The surface current (7 m) at mooring 9 was nearly due east with a speed of approximately 13 cm/s (see Figure 4). This water was being advected into filament A. This interpretation is consistent with the discussions on Figures 3, 4, 5, 6, and 7. The chlorophyll feature observed by the OCS was located south of filament A and north of filament B. The *Columbus Iselin* data collected south of 30°N show two additional surface pigment maxima aligned in the alongshore direction. Ostensibly, these were associated with filament B. With the ship progressing southward and the feature moving northward, the mapping provided a somewhat distorted picture of the feature.

The *Eastward* section was at the southern extreme of the OCS and CZCS coverages. The line of moorings 7–10 was located along this transect. Mooring 7 was in 15 m of water, 8 in 28 m, 9 in 40 m, and 10 in 75 m. Their locations are indicated in Figure 10a. In the *Eastward* data (Figure 13b), it is apparent that a major intrusion of subsurface Gulf Stream water had upwelled across the shelf and that there was enhanced upwelling near the coast as indicated by the doming of the 19° isotherm. The Gulf Stream front was located over the shelf break and its width (the distance between the 20° and 24° isotherms) was about 30 km. The surface chlorophyll values at the stations along that transect are given in Figure 13b. Again, the high chlorophyll band observed by the OCS, CZCS and the *Columbus Iselin* was found in the vicinity of 22° and 23° water, near the 105-km point. The surface salinity at that station was 36.2‰. Contrasting the *Columbus Iselin* and *East-*

ward sections, the 19° water in the northern locale upwelled to just onshore of the shelf break. Also, there was a doming of the isotherms at the shelf break in the north, but not so to the south, supposedly because of the presence of the Gulf Stream front. Filament B was to the south of 30°N and did not appear in the *Eastward* section on April 15.

3. DISCUSSION

3.1. Alongshore Variations in the Bottom Intrusion

The wind stress and sea level at Savannah during this period are given in Figure 14. The winds were highly coherent between Daytona Beach, Jacksonville, and Charleston, and alongshore variability in hydrography cannot be attributed to spatial variability in the wind stress. Offshore wind stress values are much greater than the coastal magnitudes [Lee and Atkinson, 1983]. The winds were strongly upwelling favorable from April 7 through 9 and again from April 12 to 15. Sea level response lagged behind the winds by 1–2 days and dropped sharply to –28 cm during the second wind event. On April 15, coastal upwelling was also evidenced by the elevated 19° isotherm in the *Eastward* section, by the onshore bottom currents at moorings 1, 8, 14, and 20 (Figure 1) and by the high surface chlorophyll concentrations near the coast observed in the *Eastward* data and the CZSC imagery. The bottom instrument on mooring 7 had failed and the data from moorings 13, 17, 18, and 19 are unavailable. The high pigment values along the coast can be attributed to two sources, runoff and phytoplankton response to nearshore upwelling. According to Blanton and Atkinson [1983], the April runoff was high, so both sources were active. All surface velocities in the current meter array had northward components during this wind event, but there is no evidence that the material originated from south of Cape Canaveral. On April 15, the surface current at mooring 7 had a heading of 30° from north at about 14

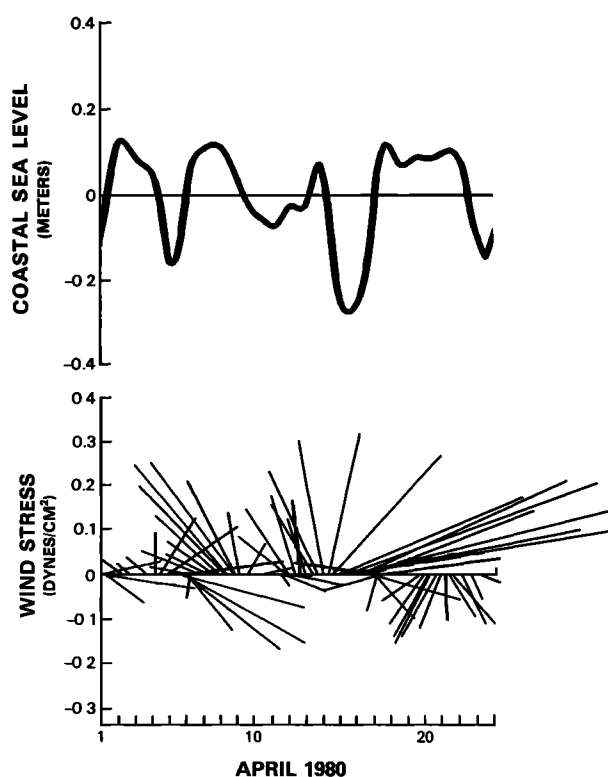


Fig. 14. Sea level and wind stress at Savannah, April 1980.

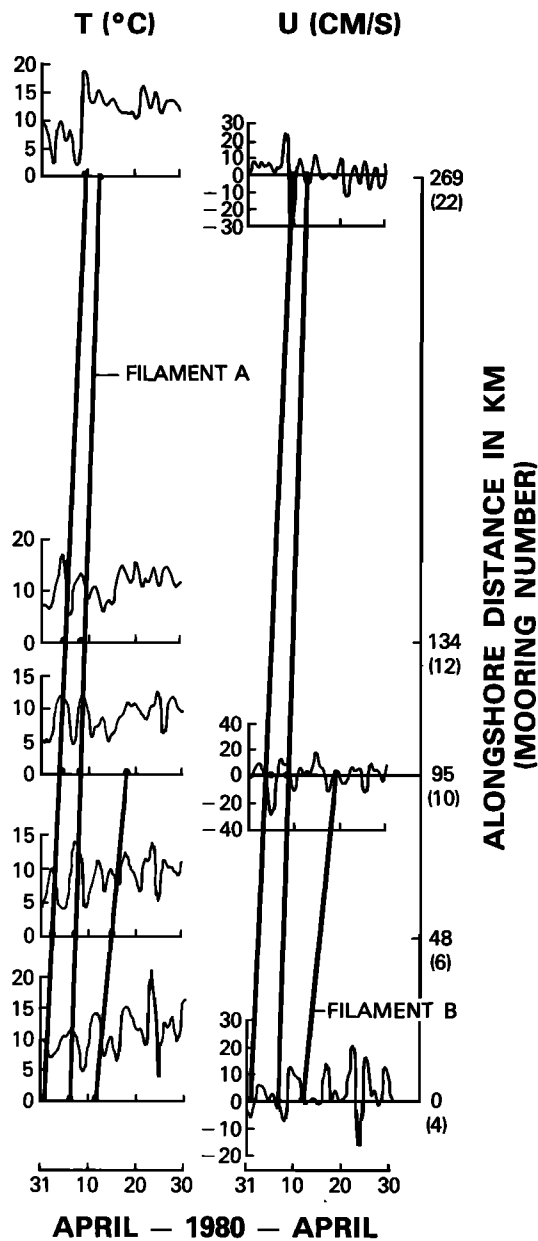


Fig. 15. Temperature and across shelf component (u) of currents during April 1980 at the 75-m moorings.

cm/s, and, as mentioned earlier, the surface current at mooring 9 was 13 cm/s at 65° (the surface meter on mooring 8 had failed). This information implies that the material being advected offshore in the narrow extrusion observed in Figure 10a was being introduced and/or produced locally and was not being advected southward along the coast. The extrusion was just to the north of filament B and is present in the other CZCS scenes (Figure 10a shows it most clearly). Finally, since the Gulf Stream south of 30°N was positioned over the shelf break, it is quite possible that the wind-driven effects were enhanced by the divergent isobath mechanism.

The bottom currents in Figure 1 at moorings 3, 4, 5, 6, 10, and 12 resemble the flow pattern described by Blanton *et al.* [1981]. The current meter data at mooring 11 were invalid according to T. Lee (personal communication, 1983), and those at 16 are unavailable. Blanton *et al.* concluded that water which had intruded onshore near Cape Canaveral exited the shelf between 30° and 31°N. They attributed this

TABLE 3. Propagation of Filament A

	Source	Cold Core		Bifurcation Point	
		North Latitude	West Longitude	North Latitude	West Longitude
April 11	CZCS	31°	80°	29.75°	80.25°
April 14	NOAA	31.25°	79.75°		
April 15	CZCS	31.50°	79.25°	30.92°	79.83°
April 16	CZCS	32°	79°	31.33°	79.75°
	NOAA	31.75°	79°		
April 17	CZCS	32.17°	78.25°	31.58°	79.58°
Estimated Propagation Speeds, cm/s					
		Cold Core		Bifurcation Point	
April 11–15		26		39	
April 11–16		33		42	
April 11–17		41		41	
April 14–16		52			
April 15–16		70		54	
April 15–17		69		45	
April 16–17		84		37	
Average		54		43	

offshore bottom flux to current-bathymetry interaction (convergent isobaths). Unfortunately, there was no hydrographic section between moorings 12 and 16 on April 15. Figure 10 indicates that mooring 12 was situated between filaments A and B, and the frontal chlorophyll feature moved past mooring 12 on April 15. The strong offshore bottom flow at mooring 12 was a maxima and was coupled with a sharp negative spike (7°C) in the temperature record. This combination of extremes in bottom temperature and the u component propagated past all the outer shelf moorings (4, 6, 10, 12, 22, and 25) and will be discussed in more detail later.

In the vicinity of the *Columbus Iselin* transect, the shelf is broader and the isobaths are convergent. There was no major bottom intrusion of upwelled Gulf Stream water, but there was a doming of isotherms at the shelf break. The bottom currents at moorings 20–22 were somewhat onshore, and the Gulf Stream front and filament B were offshore of the shelf break as indicated in Figures 10a, 11, and 13. The doming

TABLE 4. Propagation of Filament B Cold Core

	Source	Location of Cold Core	
		North Latitude	West Longitude
April 11	CZCS	29°	80.17°
April 11	NOAA	28.50°	80°
April 12	CZCS	29.50°	80.17°
April 14	NOAA	29.75°	80°
April 16	CZCS	30°	80.25°
April 16	NOAA	29.75°	80°
Estimated Propagation Speed, cm/s			
April 11–12		64	
April 11–14		54	
April 11–16		32	
April 11–16		26	
April 12–16		16	
April 14–16		0	
Average		32	

TABLE 5. Estimated Wavelengths

Filaments*	Source	Date	Estimated Wavelength, km
1-A	CZCS	April 11	146
1-A	NOAA	April 14	148
A-B	CZCS	April 11	223
A-B	NOAA	April 14	168
A-B	CZCS	April 16	252
A-B	NOAA	April 16	242

*1 refers to the feature north of filament A.

occurred at about the 45–55 m isobath and had a width compatible with the Janowitz-Pietrafesa theory. However, their theory also predicts a nearshore dome which propagates offshore as the upwelling develops. While being present to the south, it did not exist in the northern end of the bight. Also, just north of mooring 22, the Gulf Stream deflects to the east. It is suggested that the differences in the hydrography in the two sections reflect the changes in the balances between the wind, current-bathymetry, and Gulf Stream wave-induced circulations. It can be assumed that the wind would produce a uniform tendency for upwelling, while the current-bathymetry interactions induce upwelling south of 30°N and downwelling to the north. The meander induces a bottom upwelling in the trough.

3.2. Filamentary Propagation and Circulation

In Figure 15, the temperature and across-shelf (u) velocity component from the 75 m moorings are given for the month of April. The instruments are 4-2 (45 m), 6-1 (17 m), 10-2 for T (17 m), 10-1 for u (7 m), 12-1 (17 m), and 22-1 (17 m). The surface meter on mooring 4 had failed. Certain events can be tracked as they propagated through the array and their phase speeds estimated. Three of these are identified by straight lines, the first being the northernmost filament shown in Figures 8 and 12, the second is filament A, and the third is filament B. Note that every temperature peak is preceded by a decline in the u component. The slope of the lines represent the mean phase speeds of the waves while propagating through the mooring array. This method implies that the first event moved at about 39 cm/s, while filament A moved at about 50 cm/s. Table 3 provides the locations of the cold core of filament A and the estimated speeds by using the satellite imagery. The results indicate an acceleration of the feature was occurring as it approached the Charleston Bump area. Data in *Legeckis* [1975] show the same trend. The average value determined from Table 3 is 54 cm/s, which is very similar to the 55 cm/s value cited by *Lee and Atkinson* [1983] as typical of the entire GABEX data set.

The most notable characteristic of filament A is the pigment pattern within the warm tongue. In comparing the visible and

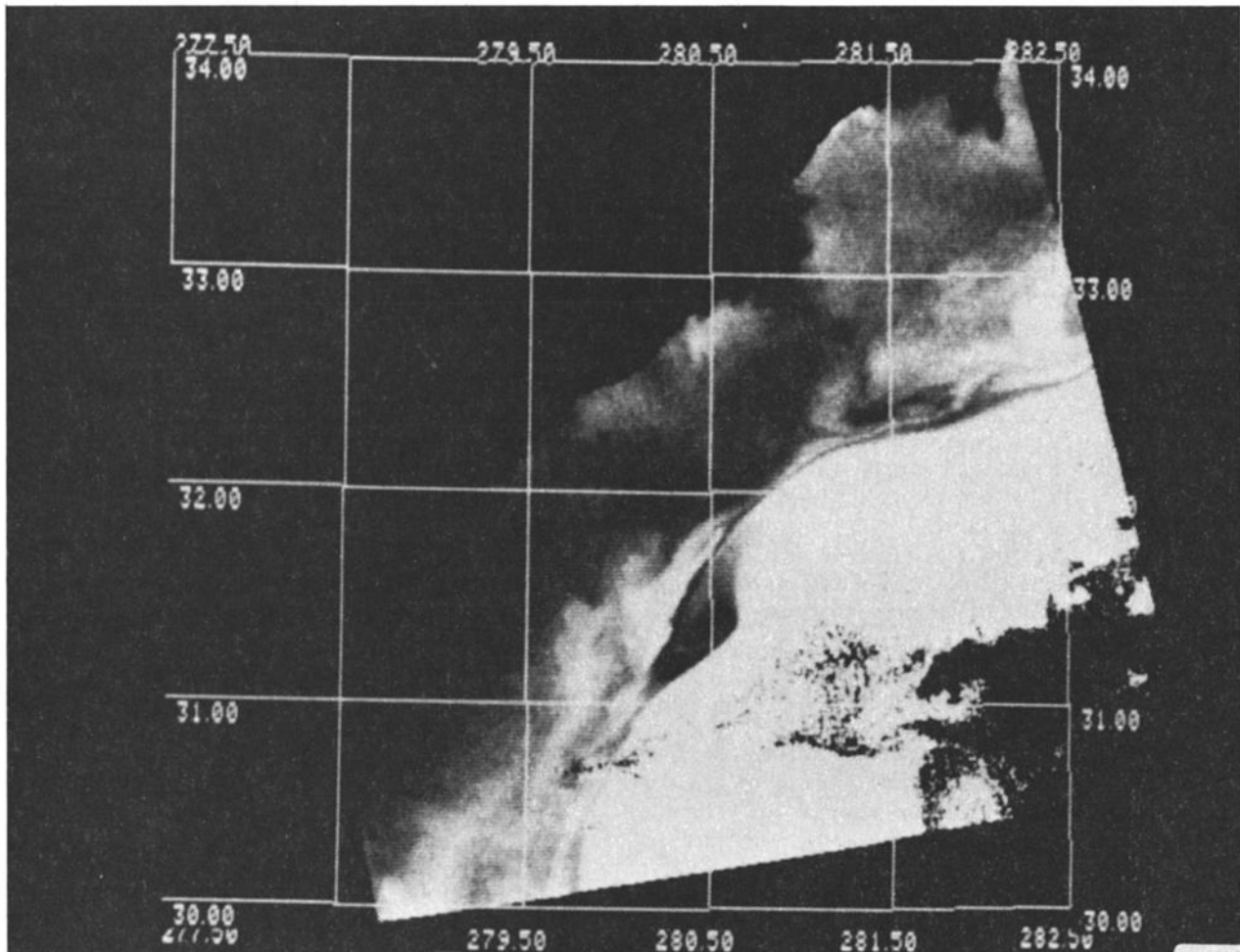


Fig. 16. CZCS enhanced visible image, April 17, 1979.

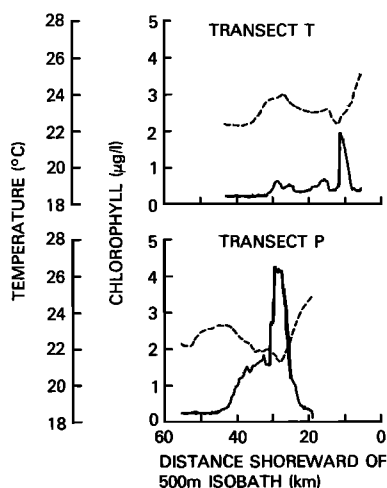


Fig. 17. Transects of surface temperature (dashed line) and chlorophyll (solid line) across a Gulf Stream filament from Yoder *et al.* [1981].

IR CZCS images (Figures 8, 10, and 11), the warmest water within the warm tongue is bounded on each side by narrow bands of pigment which merge at the southern tip of the warm tongue. This location will be referred to as the bifurcation point. This pattern was maintained during the entire period of April 11–17, and the bifurcation point can be identified in the CZCS imagery on April 11, 15, 16, 17. Table 3 gives its location on those days and the speed of its movement as estimated from various combinations of locations and times. The mean estimate is 43 cm/s. These differences in the propagation speeds of the leading and trailing points of filament A indicate that the warm tongue was lengthening at an average rate of 11 cm/s during April 11–17.

A similar analysis of the movement of filament B (Table 4) indicates a continual slowing of its motion. In fact, the NOAA analyses from April 14 and 16 imply almost no displacement. The data shown in Figure 15 indicate a mean speed past moorings 4, 6, and 10, equal to 16.4 cm/s. In Figure 8, filament B is just south of mooring 4 on April 11. The temperature at mooring 10 exhibited a gradual increase beginning on about April 14, which peaked on about April 18, suggestive of a slow moving feature. On April 16, filament B was in the vicinity of mooring 10 (Figure 11). To compare the mooring data and Table 4, it is appropriate to use data that best spans the period of April 11–18. By using the last five entries in Table 4, the mean phase speed was 25.5 cm/s. There are differences in the two methods. The speeds in Tables 4 and 5 are determined from the locations of the northern end of the cold cores, while the temperature peaks in Figure 15 tag some point within the warm tongues. Also, the use of all combinations of satellite locations to determine average speed is not exactly analogous to the slope of a line in Figure 15 when speed is changing, but, with so few data points, no other method seemed better.

Table 5 lists the various estimates of the distances between filament cold cores. In general, the NOAA analyses and the CZCS imagery are consistent. If one assumes that the mean distance between filaments A and B was the wavelength of filament B (221 km) and averages the mooring and satellite estimated speeds (24 cm/s), a comparison with Orlanski's values of 220 km and 25 cm/s for the most unstable wave is striking. However, this comparison may not be quite valid because filament B was a nonlinear wave, did not have a

constant phase speed and was shoaling on the cape, a process discussed in Lee *et al.* [1981]. The NOAA analysis on April 18 does not show filament B. Thus, the feature had deteriorated to the point that it could no longer be identified in either the satellite or the mooring data.

The surface pigment and temperature patterns observed in filaments can be quite different and may represent differences in their surface circulations. Filaments A and B exemplify contrasting patterns. Figures 8 and 9 show that surface water from the warm tongue of filament B was being entrained into the cold core region. This recirculation of warm water is similar to that suggested by Lee [1975] where it was argued that the cold core is a vortex that advects along the front, wrapping Gulf Stream water around it in a manner similar to a warm-core ring entraining slope water. However, the warm water in this case partitioned the cold core into two sections and did not encompass the entire cold core; it did not reattach to the Gulf Stream at the southern end of the cold core. The fact that entrainment occurred does not imply that anticyclonic flow did not exist in the warm tongue. Mooring 4 was the only one clearly within the warm tongue, but the surface current meter had failed. Figure 8 indicates that the southern end of filament B was very bulbous and the Gulf Stream front south of the filament (Figure 9) was positioned much closer inshore than off Cape Canaveral. Apparently, the Gulf Stream offshore of Cape Canaveral was being sharply deflected to the east as the filament was moving past the cape. Figure 15 implies that filament B was situated near mooring 4 on April 11 and 12. Therefore, it is possible that the northward winds coupled with the topographic constrictions of Cape Canaveral produced a more complicated surface flow pattern than those of the filaments found farther north. In contrast to filament B, the pigment pattern of filament A suggests an anticyclonic flow within the warm tongue. If the sources of the phytoplankton were the cold core and the extruded waters from the south which were being advected along the front into filament A,

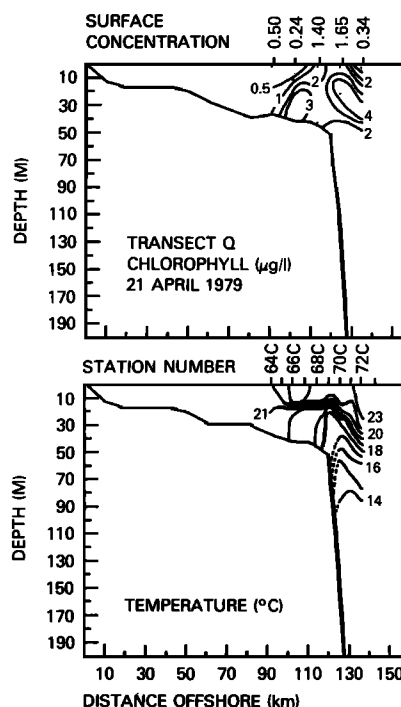


Fig. 18. Sections of chlorophyll and temperature across a Gulf Stream filament from Yoder *et al.* [1981].

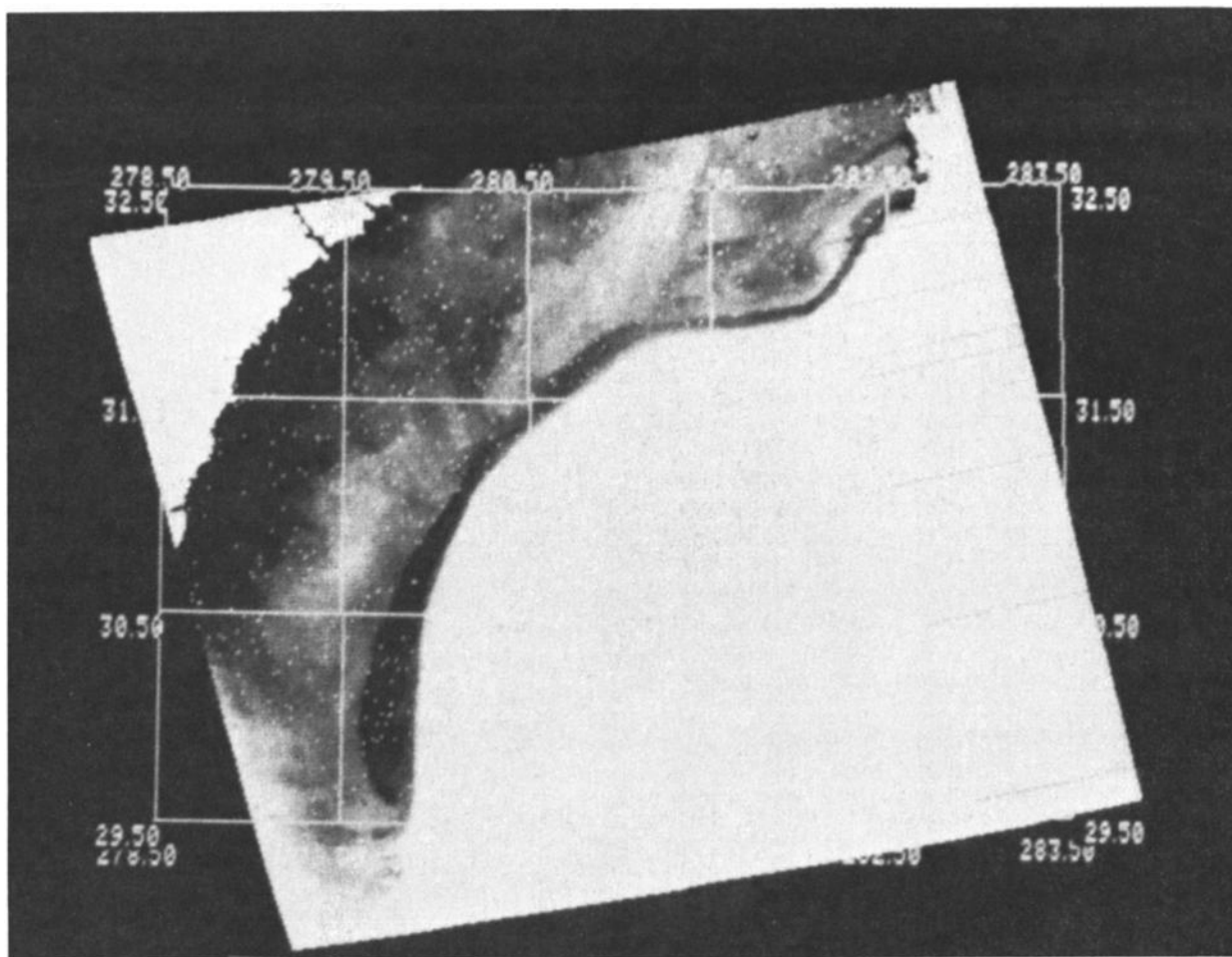


Fig. 19a. CZCS visible image, April 28, 1979. White specks are data dropouts.

then no other circulation would produce such a pattern and maintain it throughout the strong wind event which commenced on April 12.

Other examples of surface pigment patterns similar to that of filament A can be found. The circulation scheme in Figure 2 can be used to explain the patterns of three filaments observed in April 1979. Figure 16 is an enhancement of channel 1 from the CZCS on April 17. This filament had a very well defined cold core and a narrow band of relatively high chlorophyll water extending around the warm tongue from the southern end of the cold core. A similar pattern in a different filament was found on April 20 by Yoder *et al.* [1981]. This filament was obscured by cloud cover. Two of their surface mapping tracks across that feature are provided in Figure 17. Transect T crossed the northern end of the cold core, while transect P crossed the southern end of the warm tongue. Note the symmetry in the pigment distribution across the warm tongue in transect T. Section Q was north of transect P and is given in Figure 18. In this section, a high subsurface pigment layer existed between the upwelled 20° and 23°C isotherms within the cold core. Transects R and S did not extend the entire distance across the warm tongue. In transects Q and T, bands of high surface chlorophyll were found on each side of the warm tongue, while the chlorophyll maximum was located in the cold core just as observed in the April 17 filament. Transect P, evidently, was just south of the bifurcation point. If

flow within the warm tongue were entirely to the south, the narrow band of pigment along the western edge would not be attached to the cold core which was the only possible source in this case.

As a final example, the CZCS imagery from April 28 of the filament observed by Kim *et al.* [1980] is presented in Figure 19. The surface pigment and temperature profiles and the nitrate and temperature sections sampled on April 28 along a track across the feature are shown in Figures 20 and 21, respectively. In Figure 20, a comparison of CZCS pigment concentrations and shipboard fluorometer values is provided. The agreement is obvious although the observations were separated by roughly 8 hours and the transects are not coincident in space, the CZCS transect being taken south of the ship transect. An unpublished calibration algorithm by H. R. Gordon and O. B. Brown was used. In this case, the productivity was much greater than in the other cases with surface concentrations exceeding 7 $\mu\text{g/l}$. Also, the maximum concentrations occurred in the warm tongue and not in the cold core. The reason for the unusually high surface concentrations is unclear, but it is probably related to the occurrence of an intense storm which began on April 25 and continued through April 28. The winds rotated from a NW to a NE heading and exceeded 20 m/s. The high winds would have enhanced vertical mixing of nutrients from the upwelled water found within the cold core (Figures 2 and 21) which would have supported

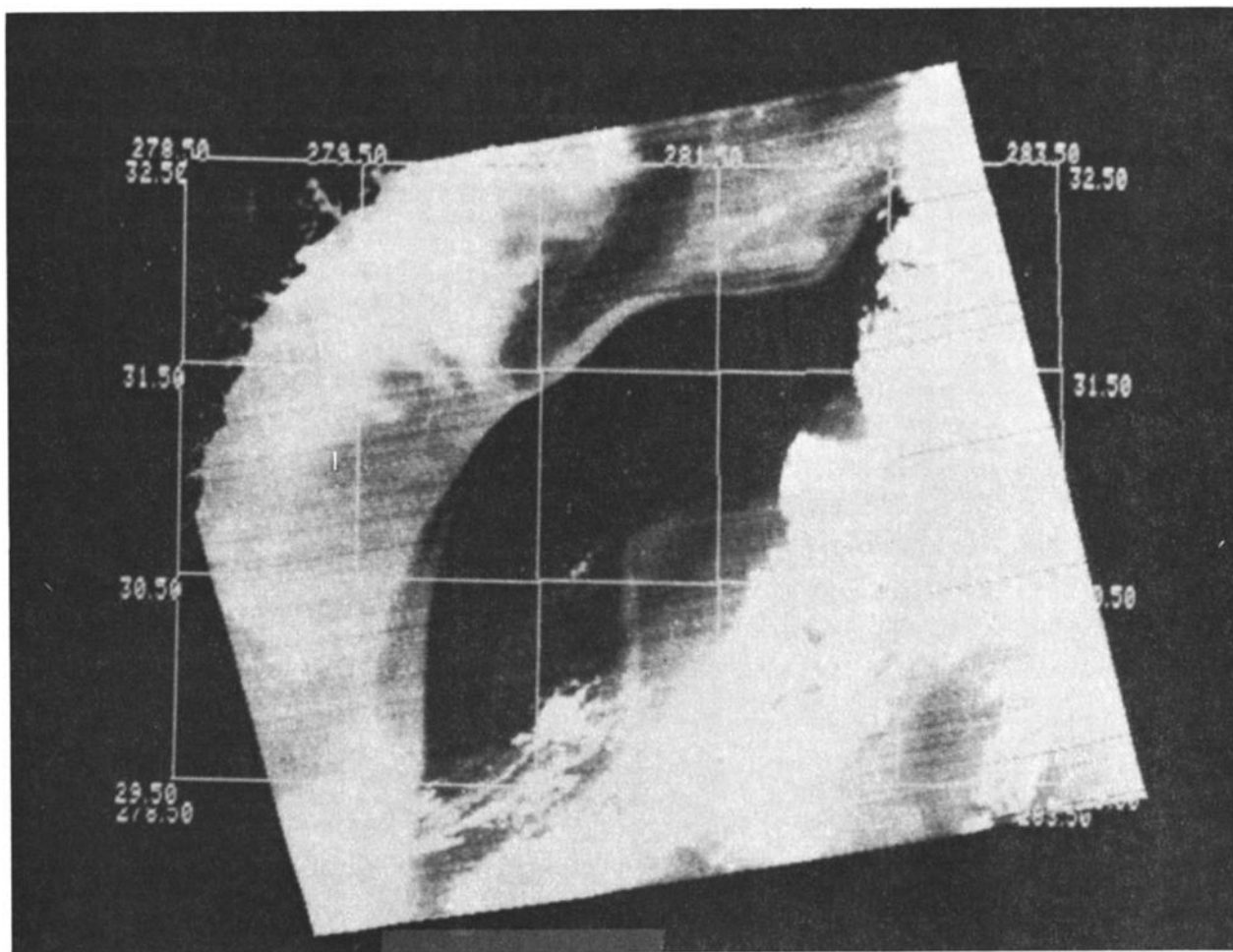


Fig. 19b. CZCS IR image, April 28, 1979.

higher concentrations of phytoplankton. The Gulf Stream front south of the filament was cloud covered, but the imagery from April 29 does not show any flux of material along the front from the south into the filament as was the case of filament A. Figure 21 corroborates the claim that the nutrients supporting the bloom were being upwelled into the cold core. A flow reversal in the warm tongue could produce the distribution in pigment concentration found in the warm tongue as well as the continuation of the chlorophyll band farther downstream of the feature. This filament and filament A were located north of Cape Canaveral and both had experienced strong northward winds just prior to the satellite coverage. Therefore, the pigment distribution in this feature could be interpreted as a more extreme case of filament A where the gap between the chlorophyll bands was closed by lateral mixing. Finally, as with filament B, an extrusion of nearshore water across the shelf was occurring just north of the filament.

3.3 Evidence of Meander-Induced Frontal Upwelling

As Figures 5, 6, and 7 indicate, within the 90-km distance between the TMS tracks, the Gulf Stream front changed from a rather broad, diffuse structure to what has been referred to as the Gulf Stream "wall." Although the northern flight track was in the vicinity of the southern end of filament A, it did not cross the filament since the track was short and was directed to that location by the ship. Also, from Figures 4 and 13, the

front was located 30–40 km offshore of the shelf break in the northern locale, while being over the shelf break to the south. This across-shelf structure is very similar to that described by Chew [1974] in his studies of the Florida Current. Chew used triads of drogues, hydrographic sections, and surface mappings to observe the structure of meanders. He found that along a meander crest, the drogues separated and the distance between surface isotherms increased, indicating a surface divergence/upwelling occurred there. The opposite behavior was found in the trough (i.e., surface convergence or downwelling). Newton [1978] postulated the same vertical motions. Chew did not make measurements of the distribution of biological quantities.

The offshore band of high chlorophyll observed by the *Columbus Iselin*, the aircraft sensors, and the CZCS on April 15 can be traced to the subsurface chlorophyll maximum within the Gulf Stream. The vertical cast at station 159 (Figure 4) on April 18 is shown in Figure 22. The subsurface maximum was between 30 and 50 m. The temperature in that depth range had a steplike structure with values between 23° and 25°C, exactly the same as in Figure 6. The concentrations are similar to those in Figure 4, the surface values being somewhat higher, as expected.

As mentioned earlier, the bottom temperature and offshore velocity component records at moorings 4, 6, 10, 12, 22, and 25 (32°33'N, 78°36'N) clearly indicate the propagation

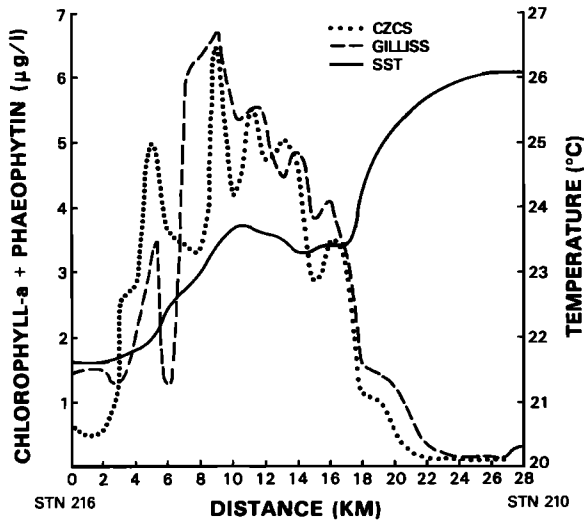


Fig. 20. Surface temperature and pigment distribution across the Gulf Stream filament as determined from the Gilliss and the CZCS on April 28, 1979.

through the bight of a rapidly moving event. It occurred in the following sequence: mooring 4 (April 13), 6 (April 13), 10 (April 14), 12 (April 15), 22 (April 16), and 25 (April 17). It closely tracked the frontal upwelling observed in the CZCS data on April 15, 16, and 17, although it is not possible to accurately determine the phasing between the surface feature and the bottom flow from the available plots. The surface mooring records do not show this event clearly, and it is not identified in Figure 15. This wave was designated as event 6 in Lee and Atkinson [1983]. The estimated elapsed time between moorings 4 and 25 is 3.5 days, resulting in an estimated speed of 137 cm/s. Table 6 provides the estimated locations of the leading and trailing ends of the bloom. Based on these, the average estimated speed is 131 cm/s.

Additional evidence of the crest's passage is the northward displacement of the front observed between April 15 and 16

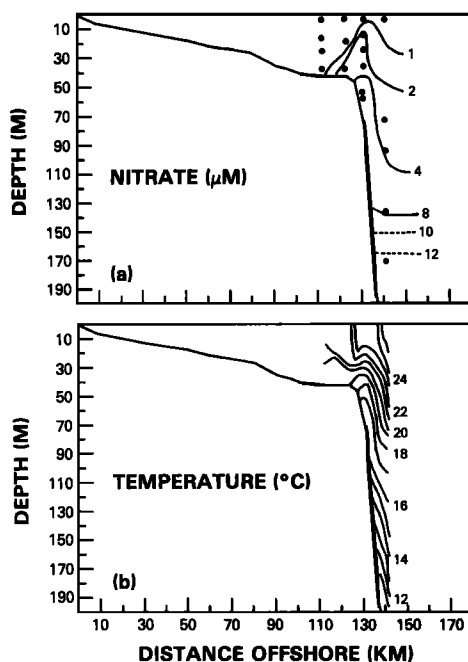


Fig. 21. Nitrate and temperature sections across the filament, April 28, 1979.

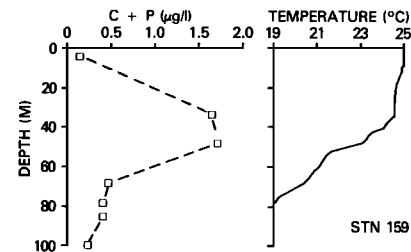


Fig. 22. Vertical profiles of temperature and pigment concentration at station 159, April 18, 1980.

along the 281st meridian (79°W). However, the front intersected the 280th meridian at the same location on both days. Between April 16 and 17, the wave was moving essentially to the east, and the front experienced a similar deflection to the north along the 282nd meridian as the bloom passed. The magnitude of these displacements averaged 25 km. The mean length of the bloom was roughly 137 km on April 16 and 17. If this distance were taken to be half a wavelength, then the wavelength would be 274 km. With characteristic wavelength and phase speed of 274 km and 134 cm/s, this meander would have a period of 2.35 days. Lee and Atkinson reported 2 and 2.5 day periodicities.

As a final note, examination of Figure 15 reveals a non-propagating peak at moorings 6, 10, and 12 between the peaks denoting the passages of filaments A and B. This peak may be superpositioned on other peaks in the other temperature records and occurred during the period of slack winds between the two wind events.

4. CONCLUSIONS

The principal purpose of this paper is to demonstrate the usefulness of ocean colorimetry to physical and biological oceanographic studies. In this particular case, the GABEX site was the scene of five different upwellings, one that was near-shore and wind driven, three that were filament induced, and a fifth that was meander generated. It is probable that the strength of the wind-driven upwelling was influenced by current-bathymetry interactions and Gulf Stream frontal events. Observations of filaments indicate that the circulation within them can vary somewhat depending on the local geometry of the shelf and, to a lesser extent, the wind. In one

TABLE 6. Propagation of Meander

Date	Location	
	North Latitude	West Longitude
April 15	30.88°	79.58°*
April 16	31.83°	79°*
April 17	32.17°	78°*
April 16	30.75°	79.92°†
April 17	31.75°	79.25°†
Meters/Dates		Estimated Phase Speeds, cm/s
4–25		137
April 15–16		138*
April 15–17		120*
April 16–17		117*
April 16–17		148†

*Leading end of bloom.

†Trailing end of bloom.

situation, filament A, the pigment pattern resembled the anticyclonic streamline pattern advocated by Pietrafesa in several publications and by Chew [1981]. In the case of filament B, the flow was more complex and resembled, in a limited way, what has been called a spin-off eddy [Lee, 1975]. Intense shoaling of filament B as it propagated past Cape Canaveral may have been responsible for its ultimate demise. The deceleration of the cold core represents one aspect of the decay process. The estimates of the phase speed of filament A, as determined from the mooring data and the imagery, are consistent with the Lee and Atkinson [1983] value of 55 cm/s. The slower speed of the bifurcation point (43 cm/s) could be interpreted as evidence that the warm tongue was lengthening at an average rate of 11 cm/s. Lee et al. [1981] report that one filament actually doubled its length in 1 day, a rate much greater than that found here. It appears that the phase speed of a wave can vary considerably with location. Filament A exhibited an increase in speed, while filament B decelerated while propagating within the Georgia Bight.

The existence of a meander propagating along the front simultaneously with the filaments is evidenced by (1) the lateral changes in the front's location with respect to shelf break as the feature progressed, (2) the presence of a zone of surface divergence and its movement downstream, (3) the connection between the surface chlorophyll and temperature fields within that zone and the vertical profiles of temperature and chlorophyll further offshore, and (4) the synchronous propagation of an event as observed in the bottom mooring array and a frontal upwelling zone at the surface.

The phytoplankton found in both the filament cold core and the meander crest do not advect at the same speed as these two areas, but are simply upwelled to the surface as the waves pass (or are passed) and are then either downwelled as part of the subsurface chlorophyll maximum or entrained into the warm tongue and remain near the surface. In fact, upwelling velocities at the shelf break can be quite large. Lee and Atkinson [1983] estimated that vertical velocities at the shelf break can exceed 10^{-2} cm/s.

One recommendation seems in order. Some questions regarding the surface circulation of filaments could be resolved by employing an aircraft and combining a PRT-5/AXB T survey as executed by Bane et al. [1981] with the Lagrangian techniques employed by McClain et al. [1982].

Acknowledgments. The authors wish to thank the following agencies which have provided support for this study: The U.S. Department of Energy, contract DOE-AS09-76EY-00902 (to L. J. Pietrafesa), contract DOE-AS09-76EV-00936 (to J. A. Yoder), and NASA RTOP 146-40-15-25 (to H. H. Kim/C. R. McClain). Some U.S. Department of Energy funding to Skidaway Institute of Oceanography (DOE DE-AS09-76V00901) was used to support the collection and analyses of CZCS data at NASA/GSFC. We are especially grateful to T. N. Lee (University of Miami) for providing current meter data and concise reviews (DOE-AS05-76EV-05163) and to L. P. Atkinson (Skidaway Institute of Oceanography) for sharing the hydrographic data (DOE-AS09-76EV-00889). Others who contributed to this work are H. H. Kim, Dave Clem, Lib Rogers, and D. B. Rao of NASA/GSFC, W. D. Hart of Science Systems and Applications, Inc., Judy Fuh of General Software Corporation, and Eileen Hofmann of Texas A&M University.

REFERENCES

- Atkinson, L. P., Modes of Gulf Stream intrusion into the South Atlantic Bight shelf waters, *Geophys. Res. Lett.*, **4**, 583–586, 1977.
- Bane, J. M., Jr., and D. A. Brooks, Gulf Stream meanders along the continental margin from the Florida Straits to Cape Hatteras, *Geophys. Res. Lett.*, **6**, 280–282, 1979.
- Bane, J. M., Jr., D. A. Brooks, and K. R. Lorenzen, Synoptic observations of the three dimensional structure and propagation of Gulf Stream meanders along the Carolina continental margin, *J. Geophys. Res.*, **86**, 6411–6425, 1981.
- Blanton, J. O., Exchange of Gulf Stream water with North Carolina shelf water in Onslow Bay during stratified conditions, *Deep Sea Res.*, **18**, 167–178, 1971.
- Blanton, J. O., and L. P. Atkinson, Transport and fate of river discharge on the continental shelf of the southeastern United States, *J. Geophys. Res.*, **88**, 4730–4738, 1983.
- Blanton, J. O., and L. J. Pietrafesa, Flushing of the continental shelf of Cape Hatteras by the Gulf Stream, *Geophys. Res. Lett.*, **5**, 495–498, 1978.
- Blanton, J. O., L. P. Atkinson, L. J. Pietrafesa, and T. N. Lee, The intrusion of Gulf Stream water across the continental shelf due to topographically-induced upwelling, *Deep Sea Res.*, **28A**, 393–405, 1981.
- Brooks, D. A., and J. M. Bane, Jr., Gulf Stream deflection by a bottom feature off Charleston, South Carolina, *Science*, **201**, 1225–1226, 1978.
- Brooks, D. A., and J. M. Bane, Jr., Gulf Stream fluctuations and meanders over the Onslow Bay upper continental slope, *J. Phys. Oceanogr.*, **11**, 247–256, 1981.
- Chao, S.-Y., and G. S. Janowitz, The effect of a localized topographic irregularity on the flow of a boundary current along the continental margin, *J. Phys. Oceanogr.*, **9**, 900–910, 1979.
- Chao, S.-Y., and L. J. Pietrafesa, The subtidal response of sea level to atmospheric forcing in the Carolina Capes, *J. Phys. Oceanogr.*, **10**, 1246–1255, 1980.
- Chew, F., The turning process in meandering currents: A case study, *J. Phys. Oceanogr.*, **4**, 27–57, 1974.
- Chew, F., Shingles, spin-off eddies and an hypothesis, *Deep Sea Res.*, **28A**, 379–391, 1981.
- Chew, F., J. M. Bane, Jr., and D. A. Brooks, The propagation of a cold-dome meander: A conceptual model, in *Proceedings Workshop on Gulf Stream Structure and Variability*, pp. 63–68, University of North Carolina, Chapel Hill, N. C., 1982.
- Clarke, G. L., G. C. Ewing, and C. J. Lorenzen, Spectra of back-scattered light from the sea obtained from aircraft as a measure of chlorophyll concentrations, *Science*, **167**, 1119–1121, 1970.
- Düing, W., Synoptic studies of transients in the Florida Current, *J. Mar. Res.*, **33**, 53–72, 1975.
- Dunstan, W. M., and L. P. Atkinson, Sources of new nitrogen for the South Atlantic Bight, *Estuar. Proc.*, **1**, 69–78, 1976.
- Gordon, H. R., and D. K. Clark, Atmospheric effects in the remote sensing of phytoplankton pigments, *Boundary Layer Meteorol.*, **18**, 299–313, 1980.
- Gordon, H. R., D. K. Clark, J. W. Brown, O. B. Brown, and R. H. Evans, Satellite measurement of the phytoplankton pigment concentration in the surface waters of a warm core Gulf Stream ring, *J. Mar. Res.*, **40**, 491–502, 1982.
- Gordon, H. R., D. K. Clark, J. W. Brown, O. B. Brown, R. H. Evans, and W. W. Broenkow, Phytoplankton pigment concentrations in the Middle Atlantic Bight: Comparison of ship determinations and CZCS estimates, *Appl. Opt.*, **22**, 20–35, 1983.
- Hill, R. B., and J. A. Johnson, A theory of upwelling over the shelf break, *J. Phys. Oceanogr.*, **4**, 19–26, 1974.
- Hofmann, E. E., L. J. Pietrafesa, and L. P. Atkinson, A bottom water intrusion in Onslow Bay, North Carolina, *Deep Sea Res.*, **28A**, 329–345, 1981.
- Hovis, W. A., The Nimbus 7 Coastal Zone Color Scanner (CZCS) program, in *Oceanography from Space*, edited by J. F. R. Gower, pp. 213–225, Plenum, New York, 1981.
- Hsueh, Y., and H.-W. Ou, On the possibilities of coastal, mid-shelf, and shelf break upwelling, *J. Phys. Oceanogr.*, **5**, 670–682, 1975.
- Janowitz, G. S., and L. J. Pietrafesa, A model and observations of time-dependent upwelling over the mid-shelf and slope, *J. Phys. Oceanogr.*, **10**, 1574–1583, 1980.
- Janowitz, G. S., L. J. Pietrafesa, The effects of alongshore variation in bottom topography on a boundary current, or, topographically induced upwelling, *Continental Shelf Res.*, **1**, 123–141, 1982.
- Kim, H. H., C. R. McClain, L. R. Blaine, W. D. Hart, L. P. Atkinson, and J. A. Yoder, Ocean chlorophyll studies from a U-2 platform, *J. Geophys. Res.*, **85**, 3982–3990, 1980.
- Lee, T. N., Florida Current spin-off eddies, *Deep Sea Res.*, **22**, 753–765, 1975.
- Lee, T. N., and L. P. Atkinson, Low-frequency current and temperature variability from Gulf Stream frontal eddies and atmospheric

- forcing along the southeastern U.S. outer continental shelf, *J. Geophys. Res.*, **88**, 4541–4567, 1983.
- Lee, T. N., and D. A. Brooks, Initial observations of current, temperature, and coastal sea level response to atmospheric and Gulf Stream forcing on the Georgia shelf, *Geophys. Res. Lett.*, **6**, 321–324, 1979.
- Lee, T. N., and D. A. Mayer, Low-frequency current variability and spin-off eddies along the shelf off Southeast Florida, *J. Mar. Res.*, **35**, 193–220, 1977.
- Lee, T. N., L. P. Atkinson, and R. V. Legeckis, Observations of a Gulf Stream frontal eddy on the Georgia continental shelf, April, 1977, *Deep Sea Res.*, **28A**, 347–378, 1981.
- Legeckis, R. V., Application of synchronous meteorological satellite data to the study of time dependent sea surface temperature changes along the boundary of the Gulf Stream, *Geophys. Res. Lett.*, **2**, 435–438, 1975.
- Legeckis, R. V., Satellite observations of the influence of bottom topography on the seaward deflection of the Gulf Stream off Charleston, South Carolina, *J. Phys. Oceanogr.*, **9**, 483–497, 1979.
- Leming, T. D., Observations of temperature, current and wind variations off the central eastern coast of Florida during 1970 and 1971, *TM NMSF-SEFC-6*, Nat. Oceanogr. Atmos. Admin., Washington, D. C., 1979.
- Leming, T. D., and C. N. K. Mooers, Cold water intrusions and upwelling near Cape Canaveral, Florida, in *Coastal Upwelling*, edited by F. A. Richard, pp. 63–71, AGU, Washington, D. C., 1981.
- McClain, C. R., N. E. Huang, and P. E. LaViolette, Measurements of sea-state variations across oceanic fronts using laser profilometry, *J. Phys. Oceanogr.*, **12**, 1228–1244, 1982.
- Morel, A., In-water and remote measurements of ocean color, *Boundary Layer Meteorol.*, **18**, 177–201, 1980.
- Newton, C. W., Fronts and wave disturbances in the Gulf Stream and atmospheric jet stream, *J. Geophys. Res.*, **83**, 4697–4706, 1978.
- Niiler, P. P., and L. A. Mysak, Barotropic waves along an eastern continental shelf, *Geophys. Fluid Dyn.*, **2**, 273–288, 1971.
- Orlanski, I., The influence of bottom topography on the stability of jets in a baroclinic fluid, *J. Atmos. Sci.*, **26**, 1216–1232, 1969.
- Pietrafesa, L. J., Survey of a Gulf Stream frontal filament, *Geophys. Res. Lett.*, **10**, 203–206, 1983.
- Pietrafesa, L. J., and G. S. Janowitz, A note on the identification of a Gulf Stream spin-off eddy from Eulerian data, *Geophys. Res. Lett.*, **6**, 549–552, 1979.
- Pietrafesa, L. J., and G. S. Janowitz, On the dynamics of the Gulf Stream front in the Carolina Capes, in *Proceedings of the 2nd International Symposium on Stratified Fluids*, pp. 184–197, Tapin, New York, 1980.
- Pietrafesa, L. J., J. O. Blanton, and L. P. Atkinson, Evidence for deflection of the Gulf Stream at the Charleston Rise, *Gulf Stream*, **4**(9), 3–7, 1978.
- Rooney, D. M., G. S. Janowitz, and L. J. Pietrafesa, A simple model of deflection of the Gulf Stream by the Charleston Rise, *Gulf Stream*, **4**(11), 3–7, 1978.
- Smith, R. C., and W. H. Wilson, Ship and satellite bio-optical research in the California Bight, in *Oceanography from Space*, edited by J. F. R. Gower, pp. 281–294, Plenum, New York, 1981.
- Stefansson, U., L. P. Atkinson, and D. F. Bumpus, Hydrographic properties and circulation of the North Carolina shelf and slope waters, *Deep Sea Res.*, **18**, 383–420, 1971.
- Sturm, B., Ocean colour remote sensing using NIMBUS 7 CZCS data, in *Oceanography from Space*, edited by J. F. R. Gower, pp. 267–279, Plenum, New York, 1981.
- Sun, C., On the dynamic variability of the Gulf Stream front, Ph.D. Dissertation, North Carolina State University, Raleigh, 1982.
- Vukovich, F. M., and B. W. Crissman, Some aspects of Gulf Stream western boundary eddies from satellite and in situ data, *J. Phys. Oceanogr.*, **10**, 1792–1813, 1980.
- Webster, F., A description of Gulf Stream meanders off Onslow Bay, *Deep Sea Res.*, **8**, 130–143, 1961.
- Yoder, J. A., L. P. Atkinson, T. N. Lee, H. H. Kim, and C. R. McClain, Role of Gulf Stream frontal eddies in forming phytoplankton patches on the outer southeastern shelf, *Limnol. Oceanogr.*, **26**, 1103–1110, 1981.
- Yoder, J. A., L. P. Atkinson, S. S. Bishop, E. E. Hoffman, and T. N. Lee, Effect of upwelling on phytoplankton productivity on the outer southeastern U.S. continental shelf, *Continental Shelf Res.*, **1**, 385–404, 1983.
- C. R. McClain, Goddard Laboratory for Atmospheric Sciences, NASA Goddard Space Flight Center, Greenbelt, MD 20771.
- L. J. Pietrafesa, Department of Marine, Earth and Atmospheric Sciences, North Carolina State University, Raleigh NC 27650.
- J. A. Yoder, Skidaway Institute of Oceanography, Savannah, GA 31406.

(Received September 12, 1983;
revised January 4, 1984;
accepted January 4, 1984.)